Research Department

Technical Report No. 74

Ocean wave forecasting in the Mediterranean Sea
A verification study in the Spanish coastal zone

A. Guillaume, M. Gomez Lahoz*, B Hansen, J.C. Carretero*

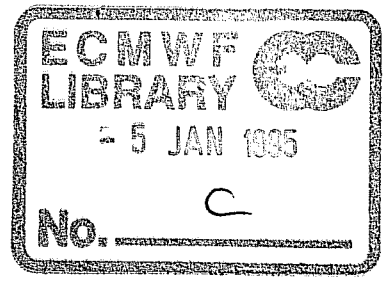

*Clima Maritimo, Puertos del Estado, Madrid, Spain

November 1994

ABSTRACT

The results of the WAM model running operationally at ECMWF for ocean wave forecasts in the Mediterranean Sea are compared against buoy observations provided by Clima Maritimo, Spain.

The verified parameters are the analysis and the 48-hour forecast of significant wave height and of mean wave period.

The verification is carried out in the Mediterranean Sea coastal zone, based on the data from three buoys, Cabopalos, Capdepera, and Palamos, the furthest off shore and in sufficient depth.

The analysis is organized to assess the relative impact of the various sources which are commonly questioned to explain discrepancies between wave model and buoy data: the accuracy of the model wind, the ability of the wave model to reproduce the physics and the dynamics of waves and the grid resolution of the wave model.

CONTENTS

1. INTRODUCTION

This paper presents some results from a verification study of the WAM model daily operational at the European Centre for Medium-Range Weather Forecasts (ECMWF) for ocean wave forecasts in the Mediterranean Sea. The verified parameters considered in this study are the analysis and the 48-hour forecast of significant wave height and mean wave period. These parameters are compared with observations from a few buoys moored in the Spanish coastal zone.

The accuracy of ocean wave forecasts is known to depend on a few main factors, which are directly related to the physics and dynamics of ocean waves and to their modelling. Waves acquire energy from the local wind. This is modelled using surface winds provided by an atmospheric model. Both the accuracy of the winds and of the wave model are involved. Waves also propagates. This implies a propagation scheme and requires a proper description of the propagating area, to correctly obtain the masking effects by coasts and islands, and, in shallow water, a proper description of the bathymetry. To summarize the accuracy of ocean wave forecasts depends on the accuracy of the model winds, of the wave model, and of the wave model grid. The relative importance of these three factors depends on the spatial scale of the meteorological phenomena that need to be taken into account.

The Mediterranean Sea is known for a high spatial and temporal variability of the wind due to the complex orography of the periphery and of the islands. Strong winds are generated by channeling in valleys, such as the Mistral from the Rhone Valley. Until recently, this variability was not obtained with operational atmospheric models, because the resolution was too coarse to approach the orography of the many mountains surrounding the Mediterranean Sea. It is only with the development of limited area model such as the PERIDOT model (*Juvanon du Vachat et al., 1987*), and with the increase in resolution of global atmospheric model, as for example to T213 for the ECMWF model, that useful results have been obtained (*Cavaleri et al., 1991, Guillaume et al., 1992*).

During the last decade, many efforts have been made to improve the observational network over the Mediterranean Sea with the extension of a buoy network, mainly by Italy and Spain, and the development of satellite observations, as for example by the altimeter from the Geosat, ERS-1 and Topex/ Poseidon satellites. For the first time, with these satellite measurements, the spatial variability of the waves in the Mediterranean Sea could be investigated (*Guillaume et al., 1992*). The new instruments are still under calibration and the buoy network remains a key element for the verification of the wave model results. Because this network has been built with the primary aim of shores and harbours protection and, also for technical reasons, the buoys are moored in the coastal zone. In the case of the Mediterranean Sea, the coastal zone is influenced by the large diurnal cycle over land and is affected by local breezes.

Several sources are thus foreseen to explain discrepancies between the wave model results and the buoy data. There is the accuracy of the model winds (orography and coastal zone effects), the ability of the wave model to reproduce the dynamics and the physics of waves and the resolution of the wave model grid. The analysis of the results of the present comparison study has been carried out to try to assess is these various sources could be separated.

The paper is organized as follows. Section 2 gives a description of the model and of the buoy results together with the verifications procedures that has been applied. We also discuss in this section some difficulties we have encountered with the different definitions of mean wave period that are commonly used. The following section presents the results of the comparison study and is organized in two parts, first an analysis on the global buoy data set, and then an analysis per buoy location. The main findings are reported in the conclusion.

2. THE VERIFICATION STUDY

The results of the WAM model daily operational at ECMWF for ocean wave forecasts in the Mediterranean Sea are compared against buoy observations provided by Clima Maritimo, Spain for the period October 1992 - February 1993. The model results are described in section 2.1 and the buoy data in section 2.2. The verified parameters are the analyses and 48-hour forecasts of significant wave height and mean wave period. Section 2.3 describes the verification procedures that have been applied and discusses the impact of the different methods that were used to define these parameters between the model and the buoy data.

2.1 WAM for the Mediterranean Sea

The Mediterranean Sea version of the WAM model (*WAMDI, 1988*) uses a grid with a 0.5 degree resolution (see Figure 1). 6-hourly analyses and forecasts of 10 meter winds from the ECMWF T213 model are used to feed the WAM model. The wave model results are available every 6 hours. For the comparison with the buoy data, the WAM model grid point the nearest to each buoy location has been selected (see Figure 1).

Following a well established practice in the wave modeling community, the significant wave height (h_s) and mean wave period (T_m) are computed from the energy density spectrum (E) according to:

$$h_s = 4\sqrt{m_0} \ , \qquad \text{(Eq.1)}$$

and

$$T_m = m_{-1}/m_0, \qquad \text{(Eq.2)}$$

where

$$m_n = \int\int E(f,\theta) f^n df d\theta \qquad \text{(Eq.3)}$$

is the n-order momentum of the spectrum.

2.2 The Spanish buoy network

The Spanish buoy network (REMRO) was created in 1960 by the Spanish Ministry of Public Works. Since 1983 the raw data measured by the buoy network are sent to Clima Maritimo (CM), now a department of Ente Publico de Puertos del Estado (the Spanish Holding of Harbours), for quality control and storage in their oceanographic data base.

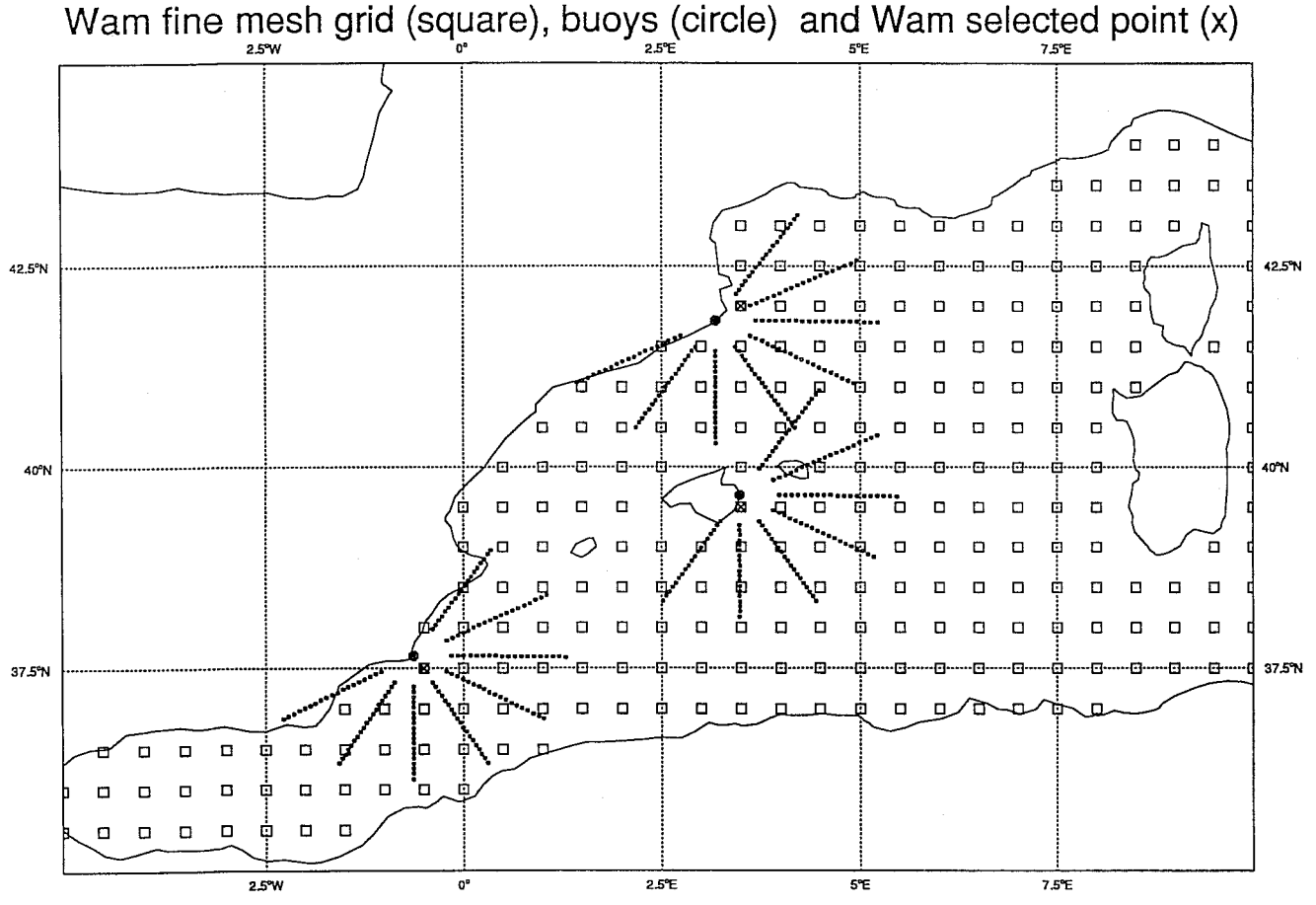

Fig 1 The WAM model grid near Spain and locations of the buoys.

Buoy locations (from South), Cabopalos, Capdepera, Palamos (circle), WAM model grid (square). The model grid point selected for the comparison is highlighted with a cross. The rays show the paths of the waves coming towards shore according to the WAM resolution of 30 °. The length of the rays gives the 12-hour travelling distance for 5 sec. period waves.

The maintenance and calibration of the buoys is regularly performed by the Harbours Laboratory following the procedures recommended by the manufacturers. The network is based on 19 scalar Datawell buoys of Waverider type, distributed along the Atlantic and Mediterranean coasts of Spain. Three additional directional buoys moored in Bilbao (Bay of Biscay), in Mahon and in Algeciras (Mediterranean Sea), although not included in the REMRO network, have also been included in the CM's data base. These three buoys are of Wavescan type and manufactured by Seatex.

For the Waverider buoys, the vertical acceleration of the buoy is measured and the signal integrated twice in order to obtain the vertical displacement. To avoid measurements of unwanted accelerations accompanying the pitch and roll of the buoy, the sensitive axis of the accelerometer is mounted on a stabilized platform, keeping the effect of horizontal accelerations below 3%. The Waverider buoy follows the sea-surface with a 1.5% accuracy for waves with frequencies ranging from 0.065 to 0.5 Hz. The measurements are transmitted every 0.5 sec to a coastal station where hourly time series of 5120 measurements are stored. The raw data are periodically sent by the stations to CM where, after quality control, they are stored in the data base.

The main aim of the REMRO network is dimensioning and protection of harbours infrastructures. Many buoys are thus located very near to the shore, in shallow water, and could not be used for the present study. Data from the only three scalar buoys located farthest from the shore and in sufficient depth, have been used: Cabopalos, Capdepera and Palamos. Cabopalos is located 2.7 nautical miles from the shore, Capdepera 1.5 and Palamos 3.5 (see Fig 1 and Annex A, for more information on the exact mooring location). Data from these buoys are also available since 1986, 1989 and 1988 respectively.

The two parameters prepared for comparison with the WAM model results are the highest one-third wave $h_{1/3}$, and the mean wave period T_z, computed following the zero-up-crossing method. The use of these two parameters is common for engineering applications and inherited from the earlier time when spectral analysis of wave records could not be easily performed. We discuss in more details in the next section, the expected differences between these buoy-derived parameters and the model ones due to the two different approaches used to compute them.

2.3 Verification procedures

From section 2.1 and section 2.2, the definitions of significant wave height and mean wave period between the model and the buoy are based on a different data analysis method. We first analyse if this might have a significant impact on the statistical results next presented.

Many experimental studies have confirm that to a first order

$$h_{1/3} \approx h_s \quad , \tag{Eq.4}$$

with some evidence that the highest one-third waves are 5% lower than the significant wave height (*Goda, 1985*) and will better verify:

$$h_{1/3} \approx 0.95\, h_s . \tag{Eq.5}$$

According to the statistical theory of random waves, the zero-up-crossing mean wave period is related to the second moment of the frequency spectrum as follows:

$$T_z = T_s \tag{Eq.6}$$

with

$$T_s = \sqrt{m_0 / m_2} \tag{Eq.7}$$

However, Eq. 6 is not as widely confirmed experimentally as Eq. 4 for the significant wave height. There have been reports that Eq. 7 produces shorter periods compared to the zero-up-crossing method, and the discrepancies do not seem to be fully understood. They could be linked to the different performances of the wave recording instruments as well as to the effect of non-linearities (*Goda, 1979*). Moreover, Eq. 7 is not the relationship that has been chosen by the WAM Group to analyse the WAM model output (*WAMDI, 1988*). Eq. 2 was preferred as a more stable parameter and a better theoretical definition of mean wave period in the context of ocean wave spectral theory.

Table 1 gives a comparison of the two definitions T_s (Eq. 7) and T_m (Eq. 2) for some Jonswap spectra,

$$E_{\mathrm{JSP}} = \alpha g^2 (2\pi)^{-4} f^{-5} \exp\left[-1.25\,(f/f_p)^{-4}\right] \gamma^{\exp\left[\left(-(f-f_p)^2\right)/\left(2\sigma^2 f_p^2\right)\right]} \tag{Eq.8}$$

with various values of peak frequency f_p and enhancement factor γ and with a shape parameter σ of 0.08 .

The T_m values are found to be up to 19% higher than the T_s values. To summarize, there are evidences that:

$$T_s < T_m \tag{Eq.9}$$

and

$$T_s < T_z . \tag{Eq.10}$$

To our knowledge, no direct comparison of T_m to T_z has been done on buoy measurements. As this would clarify some aspects of our comparison study, it was decided to perform this comparison on the buoy data set. Based on the 1D-spectra derived by Fast Fourier Transform from the buoy records, the mean wave periods derived from Eq. 2 and Eq. 7 were compared to the mean wave period obtained by the zero-up-crossing method. The results of this comparison are given in section 3.2.

f_p/γ	0.3/2.	0.3/1.	0.2/2.	0.2/1.	0.1/2.	0.1/1.
T_m (sec)	3.0	2.9	4.5	4.3	8.9	8.6
T_s (sec)	2.7	2.6	3.9	3.7	7.6	7.2
$(T_m - T_s)/T_s$	0.11	0.11	0.15	0.16	0.17	0.19

TABLE 1 Comparison of mean wave period definitions
Comparison of the two definitions $T_m = m_{-1}/m_0$ and $T_s = \sqrt{m_0/m_2}$ for some Jonswap spectra (Eq. 8). f_p is the peak frequency in Hz and γ the enhancement factor. The shape parameter σ is set to 0.08.

During the comparison the following statistical parameters have been used:

- the mean difference (or bias), i.e. the mean of the differences model minus buoy x-values,

$$\mu = \{\sum x_{mod} - x_{obs}\}/N, \qquad \text{(Eq.11)}$$

with N the number of comparison points,

- the standard deviation of the differences,

$$\sigma = \left(\{\sum (x_{mod} - x_{obs} - \mu)^2\} / \{N-1\} \right)^{1/2} \qquad \text{(Eq.12)}$$

- the scatter index,

$$SI = \sigma/\mu_{obs}, \qquad \text{(Eq.13)}$$

with μ_{obs} the mean of the observed values

- the intercept x_0 and slope λ of the linear regression, least squares fit, applied to the data set.

3. RESULTS

This section starts with the comparison of significant wave height (swh, see section 3.1) and of mean wave period (see section 3.2) for the five-months period, October 1992-February 1993 at the three buoys, Cabopalos, Capdepera and Palamos. A more detailed analysis at each buoy location is given in section 3.3.

3.1 Significant wave height comparison

At all buoy locations, the observed sea-state is on average low. The mean significant wave height is of the order of 1 m, and the maximum values are between 3 m and 5 m.

At all locations the WAM analysed swh are biased low with respect to the buoy observed swh, with biases ranging from 7 cm to 25 cm (see Table 2). Apart from Cabopalos the scatter of the differences model minus buoy is rather high, of the order of 40%. The Cabopalos buoy, where the agreement is the best with a 7cm bias and a 30% scatter index, observes the lowest sea-state with no observation of waves higher than 3 m (see Fig 2).

The model 48-hour forecast of swh (see Table 3) is also biased low compared to the buoy observations, by 6 cm to 14 cm. Compared to the buoy swh, the 48-hour forecast is less biased than the analysis, but this effect is significant at Capdepera only (14 cm instead of 25 cm). Compared to the buoy swh, the 48-hour forecast produces higher scatter indexes, 40% to 46%. However, this increase in scatter is significant at Cabopalos only, from 30% with the analysis to 40% with the 48-hour forecast.

To evaluate the impact of the wind error, and to overcome the difficulty that the winds are not measured at the buoy locations, the 48-hour wind speed forecasts are compared to the wind speed analyses (see Table 5) and the same is done for the model significant wave heights (see Table 4).

The ECMWF analysed 10 m wind speed is on averaged 5 m/s at the buoy locations. The analysed 10m wind speed is always less than 15 m/s at Cabopalos and Capdepera, and less than 20 m/s at Palamos with very few cases between 15 m/s and 20 m/s.

Compared to the analysis, the 48-hour forecast wind speeds and swh are biased high (see Table 5), but only significantly at Capdepera (0.5 m/s or 10% for the wind speed; 14 cm or 13% for the swh). At Capdepera, the mean higher waves in the 48-hour forecast are explained by mean higher wind speed in the 48-hour forecast. These higher 48-hour forecast wind speeds explain the significant lower bias found with the forecast compared to the analysis in the comparison with the buoy swh. At all locations, the 48-hour

forecast compares to the analysis with a scatter index of the same order of magnitude (see Table 4) as the one from the comparison against buoy data (see Table 3).

$h_s\,(m)$	N	$\mu_{h_{obs}}$	μ	σ	SI	h_0	λ
Cabopalos	526	0.8	-0.07	0.22	0.29	0.05	0.85
Capdepera	579	1.1	-0.25	0.42	0.38	0.12	0.65
Palamos	567	0.9	-0.14	0.41	0.44	0.12	0.72

TABLE 2 Comparison of WAM swh ANALYSIS against BUOY data.

$h_s\,(m)$	N	$\mu_{h_{obs}}$	μ	σ	SI	h_0	λ
Cabopalos	526	0.8	-0.06	0.31	0.40	0.00	0.92
Capdepera	579	1.1	-0.14	0.47	0.43	0.12	0.75
Palamos	567	0.9	-0.11	0.43	0.46	0.12	0.76

TABLE 3 Comparison of WAM 48-hour swh FORECAST against BUOY data.

$h_s\,(m)$	N	$\mu_{h_{obs}}$	μ	σ	SI	h_0	λ
Cabopalos	526	0.7	0.01	0.28	0.40	0.005	1.00
Capdepera	579	0.8	0.11	0.30	0.37	0.005	1.13
Palamos	567	0.8	0.03	0.25	0.32	0.05	0.98

TABLE 4 Comparison of WAM 48-hour swh FORECAST against WAM ANALYSIS.

$u_{10}\,(m/s)$	N	$\mu_{u_{obs}}$	μ	σ	SI	u_0	λ
Cabopalos	526	5.1	0.04	2.	0.39	1.2	0.76
Capdepera	579	5.0	0.54	2.	0.40	1.2	0.87
Palamos	567	5.3	0.00	1.8	0.34	0.9	0.82

TABLE 5 Comparison of ECMWF 48-hour u_{10} FORECAST against ECMWF ANALYSIS.

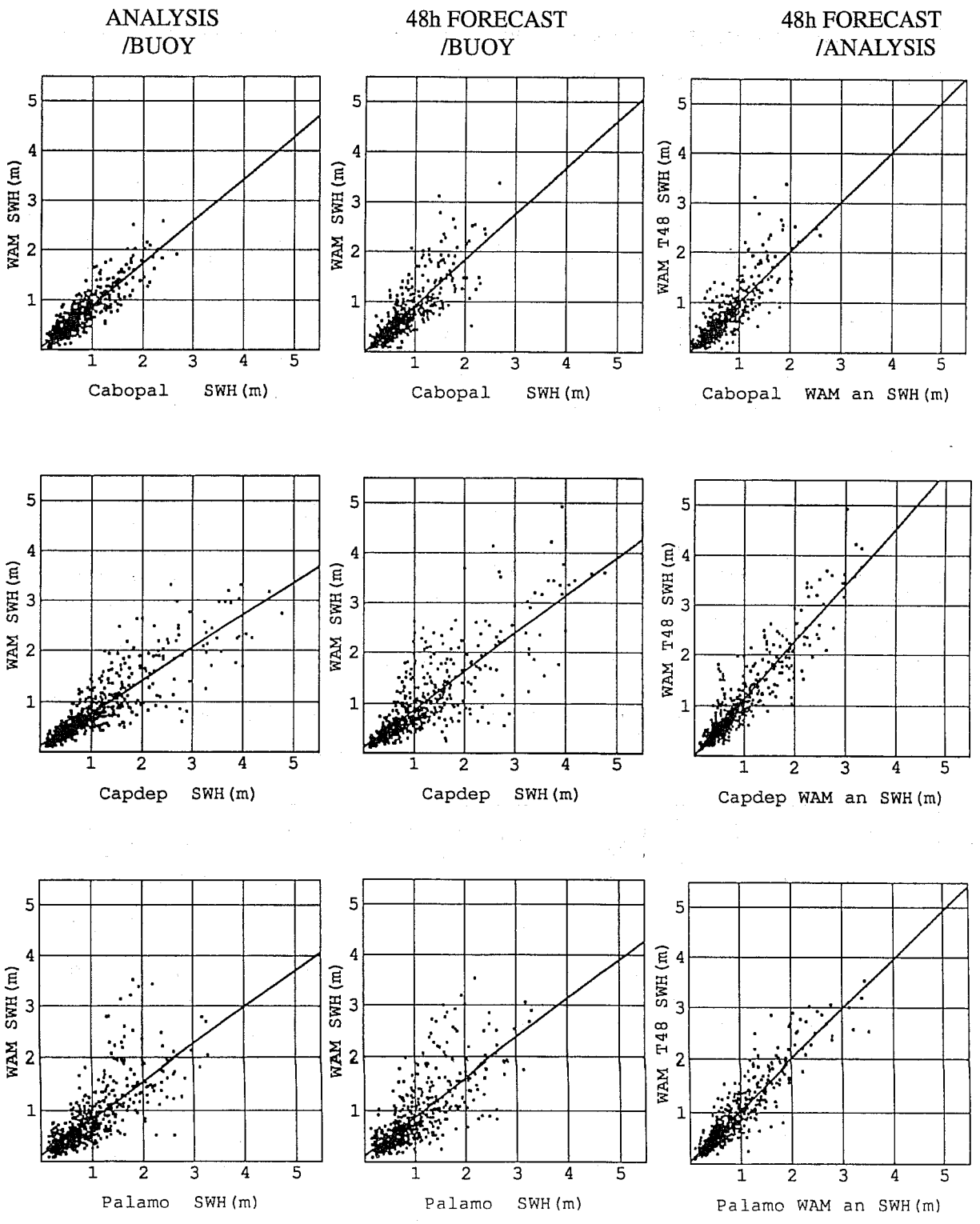

Fig 2 Comparison of significant wave height. From top to bottom: Cabopalos, Capdepera, Palamos.

48h FORECAST
/ANALYSIS

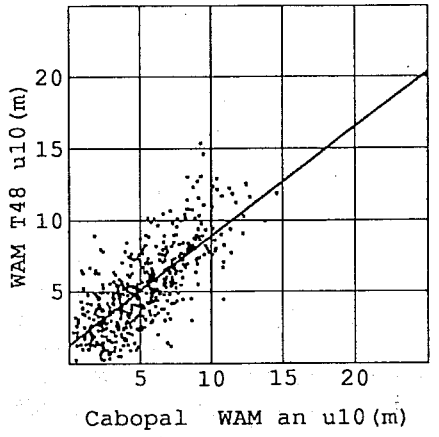

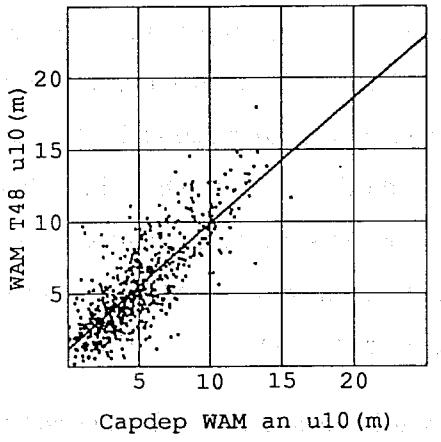

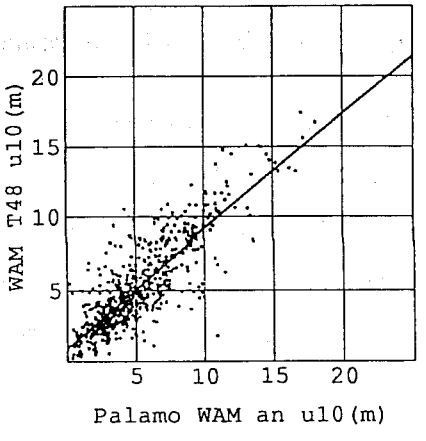

Fig 3 Comparison of 10m wind speed. From top to bottom: Cabopalos, Capdepera, Palamos.

3.2 Mean wave period comparison

To start with the three definitions of mean wave period are compared on the buoy data set. These results were obtained afterwards on a slightly bigger buoy data set now including a few missing data that had been recovered. The results are shown in Table 6.

	μ_{T_m}	μ_{T_s}	μ_{T_z}	$\mu_{T_m - T_z}$	$\mu_{T_s - T_z}$	$\sigma_{T_m - T_z}$	$\sigma_{T_s - T_z}$
Cabopalos	5.3	4.0	4.1	1.2	-0.1	0.8	0.1
Capdepera	5.7	4.6	4.7	1.0	-0.1	1.3	0.1
Palamos	5.9	4.4	4.5	1.4	-0.1	1.0	0.1

TABLE 6 Comparison of the three definitions of mean wave period on the buoy data set
$T_m = m_{-1}/m_0$ and $T_s = \sqrt{m_0/m_2}$ are derived from the 1D-spectra and T_z is the mean period defined by the zero-up-crossing method

These results confirms the preliminary results presented of section 2.3. On the present buoy data set Eq. 9 and Eq. 10 are verified, as well as Eq. 6, although that latter was questioned in the literature (see section 2.3). For the mean wave period, the definition chosen by the model and the one based on the zero-up-crossing method do not produce identical results, while the definition based on the second order momentum (Eq. 7) agree well with the zero-up-crossing definition. Compared to the zero-up-crossing method, the WAM definition produces mean wave period from 1. to 1.4 sec higher on average, with a scatter of the differences ranging from 0.8 to 1.3 sec.

The results of the comparison between the WAM mean wave period derived using the WAM definition and the buoy mean wave period derived with the zero-up-crossing method are now presented. For technical reasons, it was difficult to re-process the whole data set. Moreover, this is not necessary, as most of the results from this re-processing can be inferred using the results shown in Table 7.

With the two independent definitions, the differences between model and buoy mean wave periods are small (see Table 7) at all locations. At Palamos and Capdepera the bias is negligible, at Cabopalos the model period are on average 0.35 sec higher than the buoy ones. The standard deviations of the differences are of the same order, 0.7 sec, at all locations. Similar results are found with the 48-hour forecasts (see Table 8). Compared to the model analysis, the mean wave periods of the 48-hour forecast (see Table 9) are slightly higher. This is consistent with the findings of section 3.1 that the 48-hour wind

forecasts are stronger than the wind analyses, because with higher winds, higher waves with longer period are generated.

Based on the results of Table 7, the low biased reported in Table 7 and Table 8 in fact shows that the WAM model mean wave period are on average 1 to 1.5 sec shorter than the buoy ones. The model shorter periods, together with the model lower waves, compared to the buoy observations give a consistent picture of the behaviour of the model, namely that the model gives less developed waves compared to the buoy.

$T(s)$	N	$\mu_{T_{obs}}$	μ	σ	SI	T_0	λ
Cabopalos	526	4.0	0.35	0.73	0.18	0.91	0.86
Capdepera	579	4.7	0.01	0.76	0.16	0.49	0.90
Palamos	567	4.5	-0.04	0.72	0.16	0.21	0.94

TABLE 7 Comparison of WAM mean wave period ANALYSIS against BUOY data.
the model period is defined by $T_m = m_{-1}/m_0$, while the buoy one is obtained by the zero-up-crossing method

$T(s)$	N	$\mu_{T_{obs}}$	μ	σ	SI	T_0	λ
Cabopalos	526	4.0	0.31	0.79	0.20	0.59	0.92
Capdepera	579	4.7	0.11	0.83	0.18	0.68	0.88
Palamos	567	4.5	0.04	0.81	0.18	0.14	0.98

TABLE 8 Comparison of WAM 48-hour mean wave period FORECAST against BUOY data.
the model period is defined by $T_m = m_{-1}/m_0$, while the buoy one is obtained by the zero-up-crossing method

$T(s)$	N	$\mu_{T_{obs}}$	μ	σ	SI	T_0	λ
Cabopalos	526	4.4	0.04	0.67	0.15	0.50	0.87
Capdepera	579	4.7	0.09	0.56	0.12	0.47	0.92
Palamos	567	4.5	0.08	0.48	0.1	0.15	0.98

TABLE 9 Comparison of WAM 48-hour mean wave period FORECAST against WAM ANALYSIS.

ANALYSIS /BUOY

48h FORECAST /BUOY

48h FORECAST /ANALYSIS

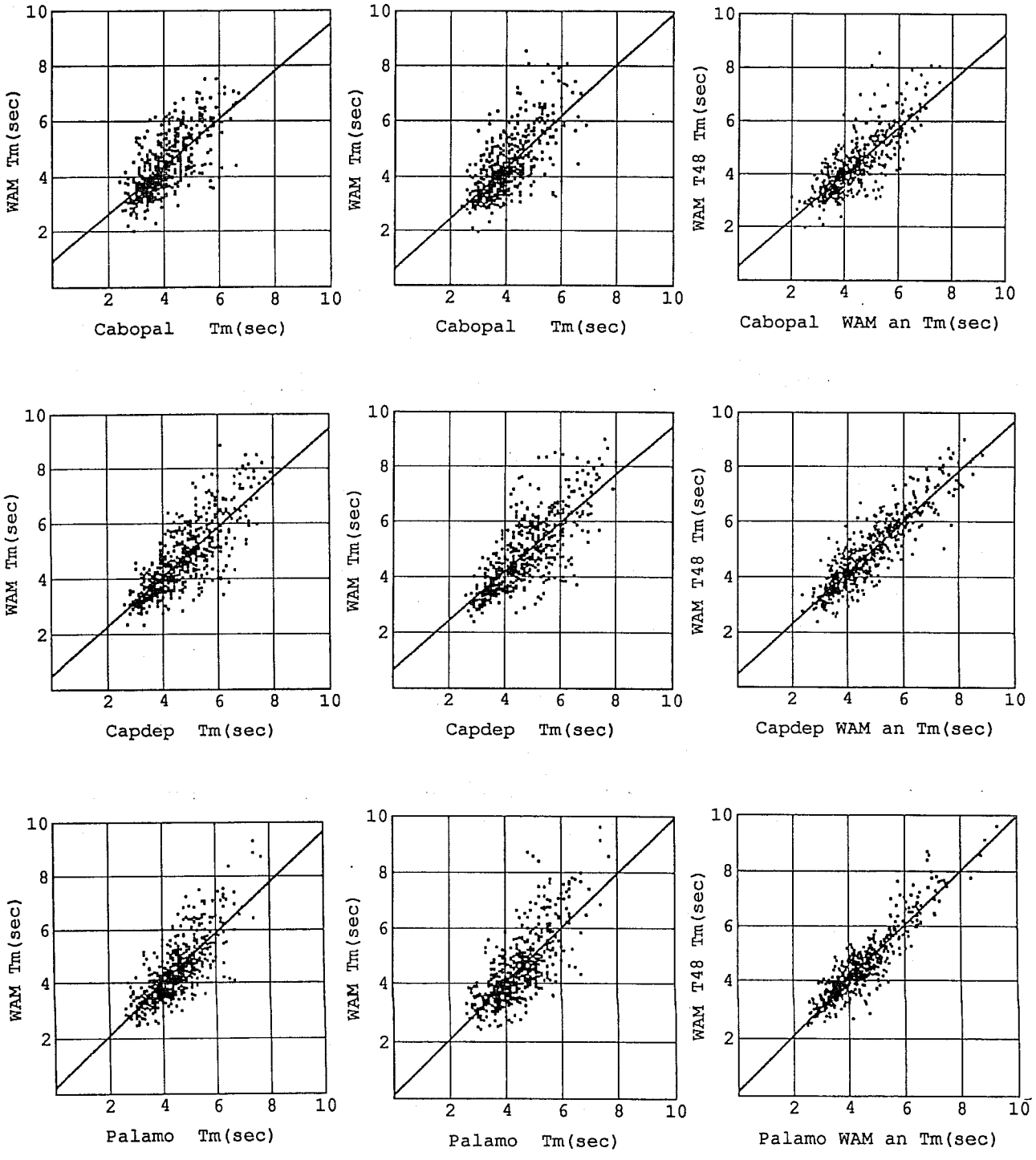

Fig 4 Comparison of mean wave period. From top to bottom: Cabopalos, Capdepera, Palamos.

3.3 Analysis per buoy location

Time series showing the evolution of significant wave height, mean wave period together with model mean wave direction, wind speed, wind direction and 2m temperature, for the whole period and at each buoy location, are gathered in ANNEX A. To analyse the various causes of the discrepancy between the model and the buoy data, we have introduced some new scatter plots (see Figures 5 to 10), which show the directional distribution of wind speed and significant wave height for the analysed and 48-hour forecasts fields. Because the wind is not measured at the buoy locations, the analysis of the wind error sources is more difficult. Moreover, because the buoy does not measure wave direction, the mean wave direction from the WAM model analysis has been used to prepare the directional distribution of buoy swh.

3.3.1 Cabopalos

At Cabopalos, the agreement between the model swh and the buoy swh is impressive, both with the analysis and 48-hour forecast (see Fig 2). On average low sea-state are observed, with no waves higher than 3m. The angular distributions of swh are also very close between the model (analysis and forecast) and the buoy (see Fig 6). The shape of the swh distribution (see Fig 6) is similar to the one of the wind speed distribution (see Fig 5), with three peaks, of directions NE, SW and NW. This indicates that the waves are mainly locally generated. In the distribution of the 48-hour forecast significantly higher easterly waves are found (see Figure 6). From Fig 5, winds stronger than 10 m/s from North/NorthEast are on averaged higher in the 48-hour forecast than in the analysis. These higher wind speeds explain the higher easterly waves in the 48-hour forecast.

3.3.2 Capdepera

At Capdepera, the directional distributions of swh does not have the same shape as the directional distribution of wind speed. This indicates a strong influence of the coast on the waves. At Capdepera, higher waves (3-5m) are observed (see Figure 2). These high waves are significantly underestimated by the wave model analysis. The 48-hour forecasts are again systematically higher than the analysis. The buoy is under the lee of Mallorca (see Figure 1 and ANNEX A) for winds blowing from SW to N, and under the lee of Menorca for winds blowing from N/NE to E/NE. It is from these directions that the model winds and waves are mainly coming. Only a few low wind are found from the remaining directions to which the buoy is fully opened, between East to South. The highest observed waves are from North (see Figure 8), they are greatly underestimated by the analysis and also, to a much lower extent, by the 48-hour forecast. With a T213 resolution, the two islands are not separated in the atmospheric model orography. Therefrom, wind channeling effects between the two islands cannot be obtained by the model. Moreover, with a 0.5 degree resolution and a 30 degree resolution in the discretization of the wave spectrum direction,

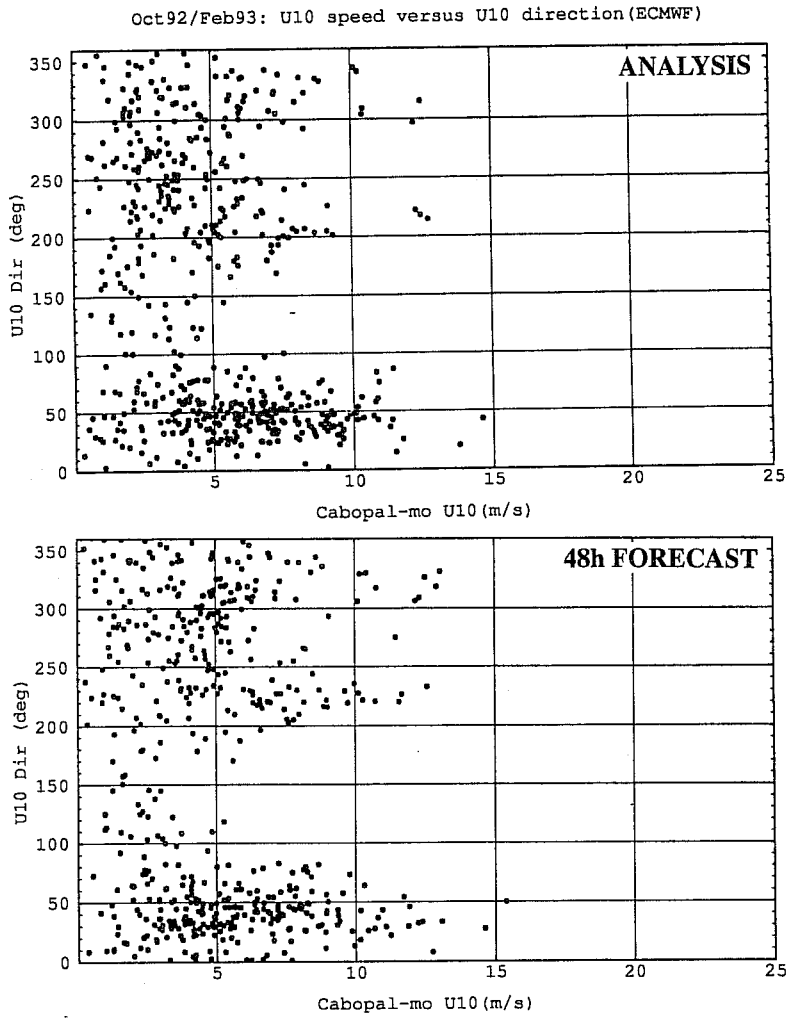

Fig 5 Angular distribution of wind speeds at Cabopalos.

Scatter plot of 10m wind direction versus 10m wind speed for the ECMWF T213 analysis (top) and 48-hour forecast (bottom).

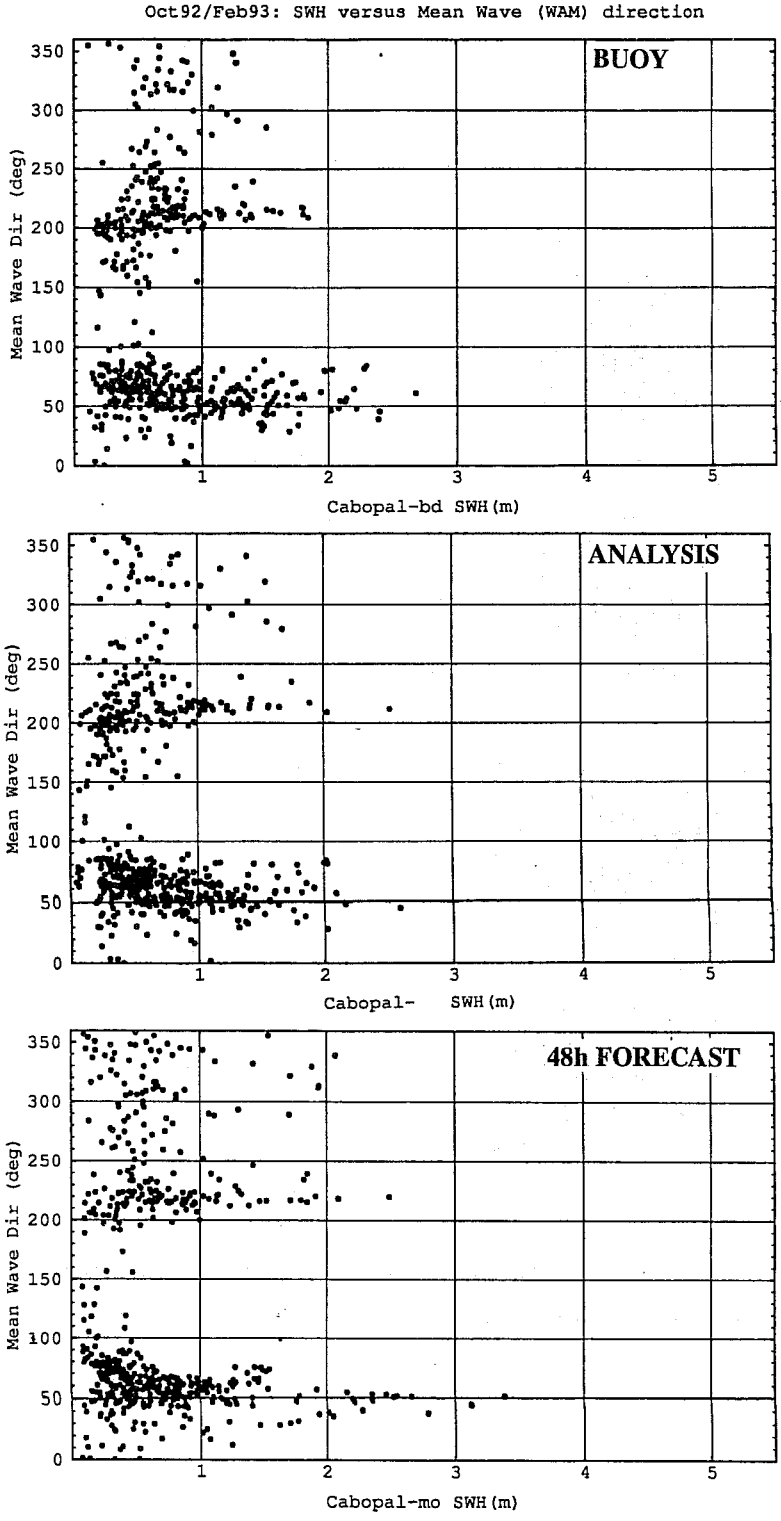

Fig 6 Angular distribution of significant wave height at Cabopalos.

Scatter plot of mean wave direction versus significant wave height. The mean wave directions shown for the buoy (top diagram) are the WAM analysed mean wave direction (the buoy does not measure mean wave direction). WAM analysis (middle diagram) and WAM 48-hour forecast (bottom diagram).

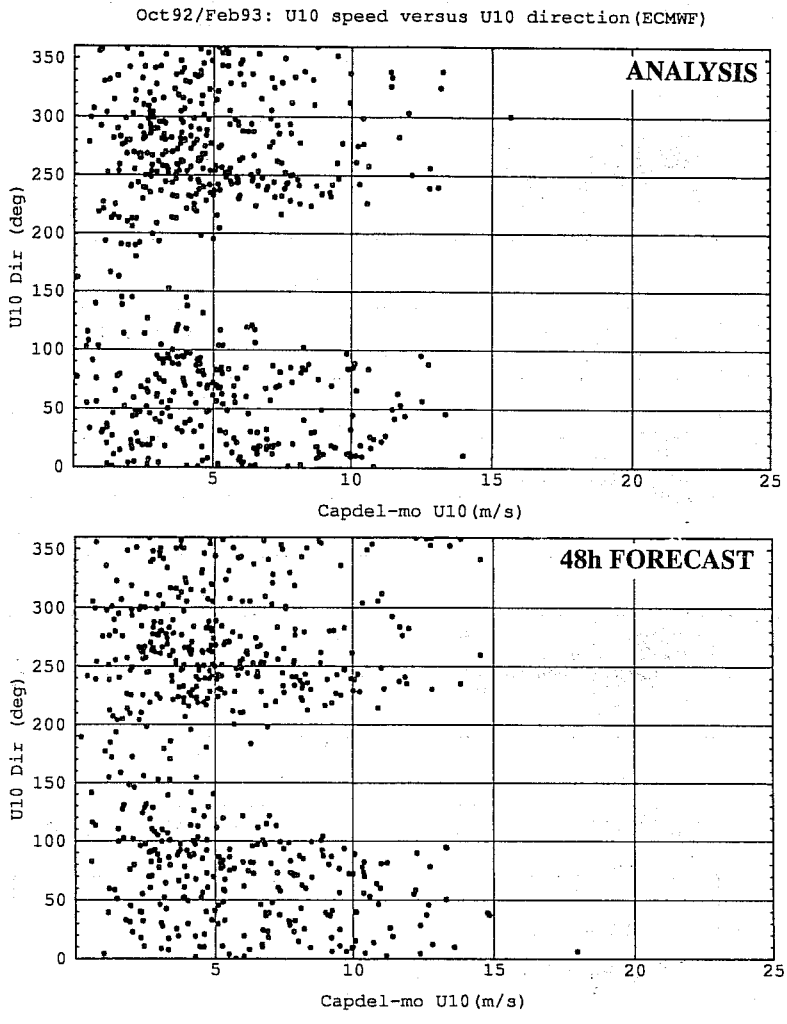

Fig 7 Angular distribution of wind speeds at Capdepera.

Scatter plot of 10m wind direction versus 10m wind speed for the ECMWF T213 analysis (top) and 48-hour forecast (bottom).

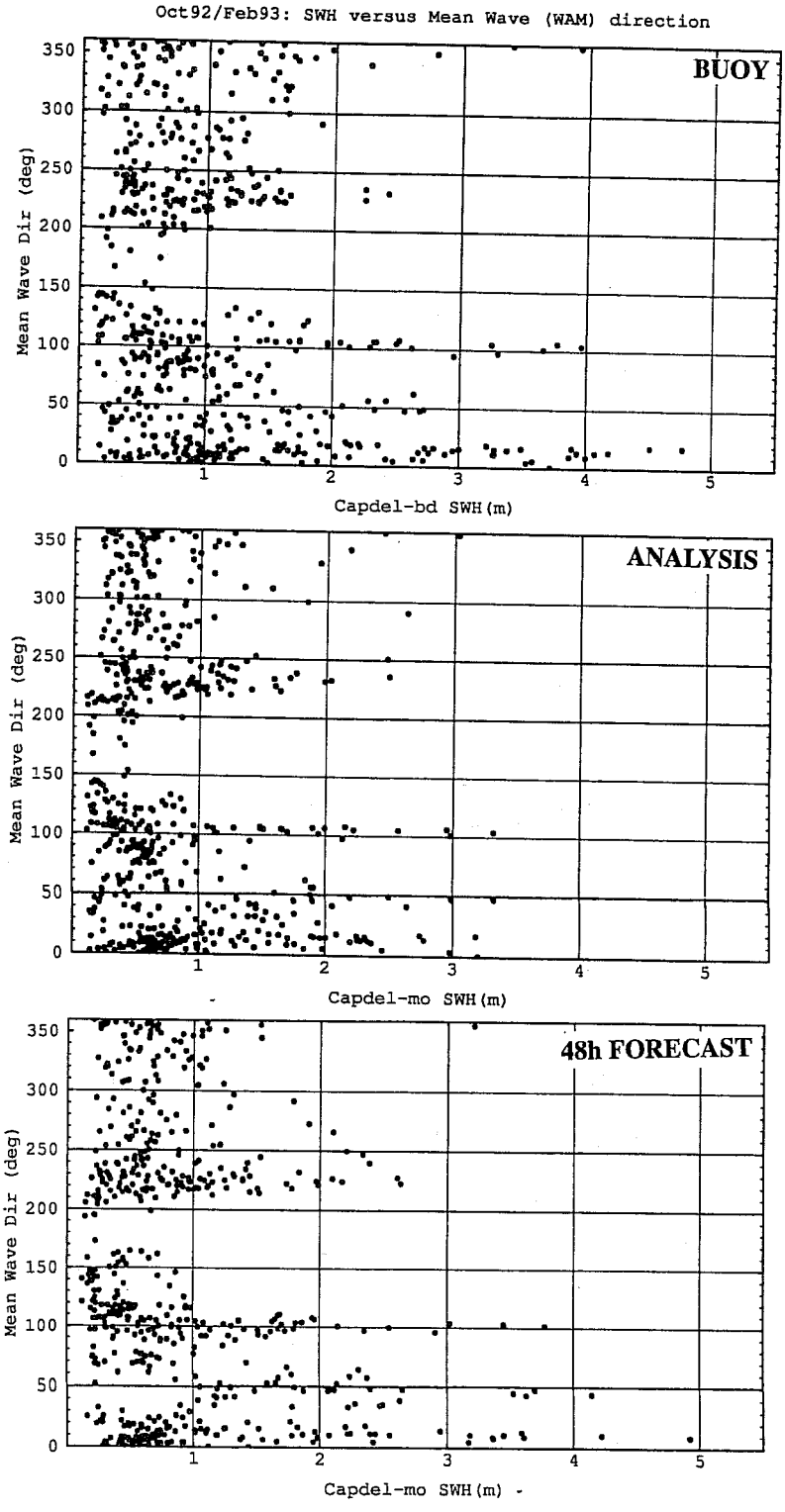

Fig 8 Angular distribution of significant wave height at Capdepera.

Scatter plot of mean wave direction versus significant wave height. The mean wave directions shown for the buoy (top diagram) are the WAM analysed mean wave direction (the buoy does not measure mean wave direction). WAM analysis (middle diagram) and WAM 48-hour forecast (bottom diagram).

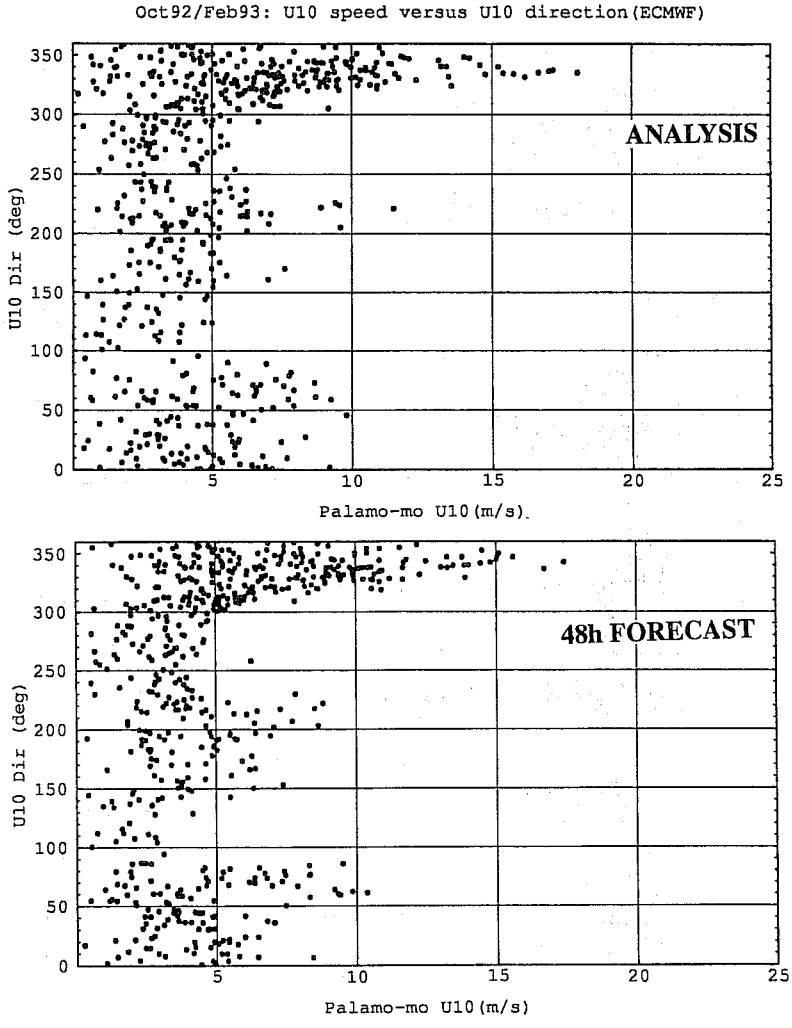

Fig 9 Angular distribution of wind speeds at Palamos

Scatter plot of 10m wind direction versus 10m wind speed for the ECMWF T213 analysis (top) and 48-hour forecast (bottom).

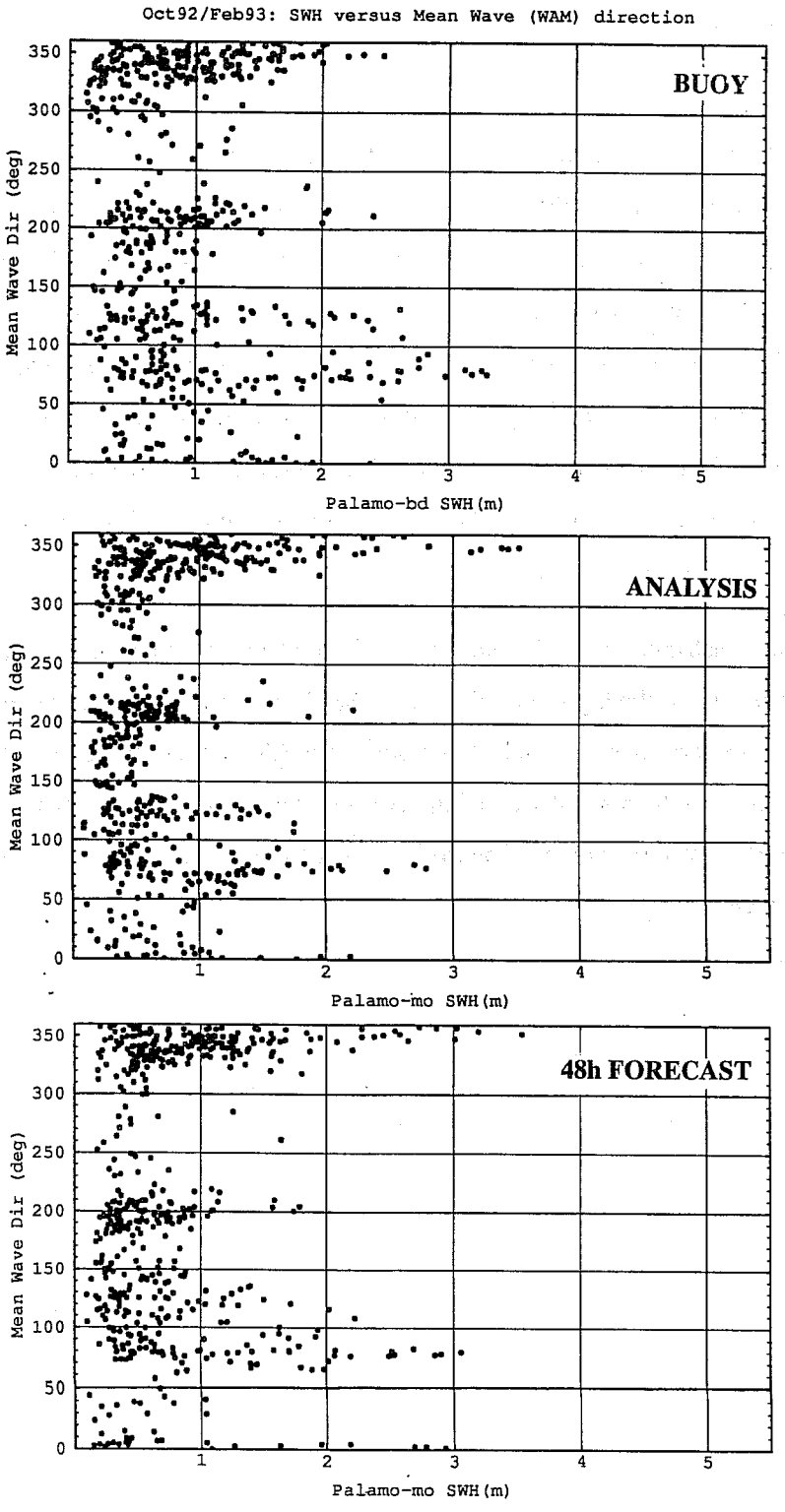

Fig 10 Angular distribution of significant wave height at Palamos.

Scatter plot of mean wave direction versus significant wave height. The mean wave directions shown for the buoy (top diagram) are the WAM analysed mean wave direction (the buoy does not measure mean wave direction). WAM analysis (middle diagram) and WAM 48-hour forecast (bottom diagram).

the WAM model encounters similar difficulty to obtain the masking effects by Menorca. This explains the discrepancies obtained between the model and the buoy data.

3.3.3 Palamos

At Palamos there are also some noticeable differences between the buoy measurements and the model results, especially for October 1992 (see Fig 11). Many peak swh values are underestimated by the model, as for example on 9, 14, 18 and 20 October. In Fig 11, the highest WAM swh in an area surrounding the buoy, 1.5 ° by 2° width, have been added. Three of the four peaks are still not achieved. This indicates that the underestimation of the peaks cannot be attributed to a too coarse resolution of the wave model grid. It must either be due to a general underestimation of the peaks of storm by the WAM model, an effect that has already been reported in the Mediterranean Sea by Guillaume et al. (1992) in a comparison with altimeter observations from Geosat, and/or to an underestimation of the wind speed by the ECMWF atmospheric model.

The directional distribution of wind speed (see Figure 9) shows that the strongest winds are from N/NW. This is the direction of the highest model waves (see Figure 10) and these waves are overestimated compared to the buoy observations. The selected model point (the nearest to the buoy location) is located to the North and is closer to the main stream of the Northwesterly winds. This spatial discrepancy could easily explain this model overestimation. However, from the other directions, the swh is underestimated by the model at all ranges.

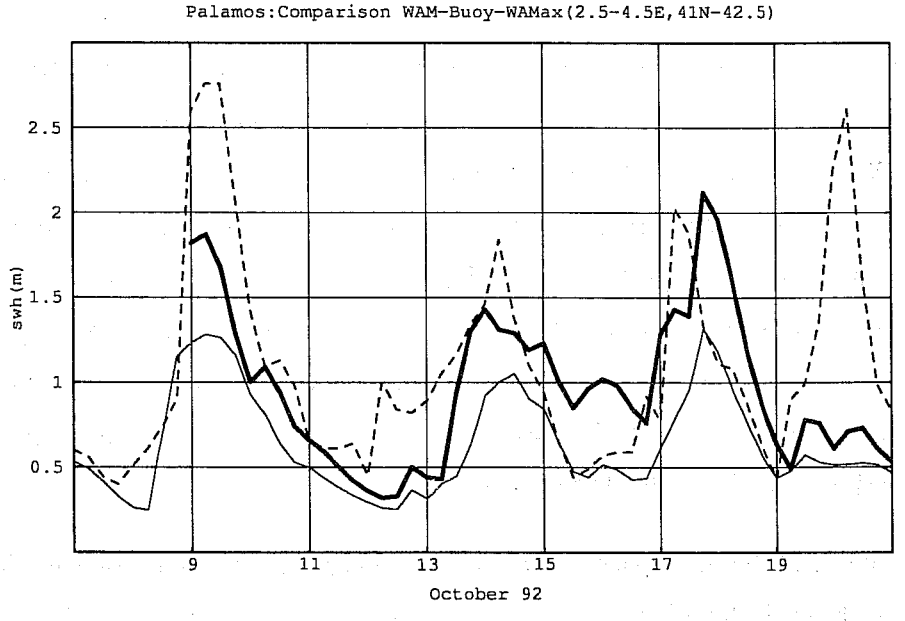

Fig 11 Palamos - October 1992: significant wave height comparison

Buoy swh (doted line), WAM swh from the nearest grid point (thin line), WAM swh the greatest in the area 2.5°E-4.5°E, 41.°N-42.5°N surrounding the buoy location (thick line).

4. CONCLUSION

Significant wave heights and mean wave periods derived from the WAM model have been compared with observations from the Spanish buoy network moored in the Spanish coastal zone.

The parameters that were compared are the significant wave height and the mean wave period. These parameters were obtained with the zero-up-crossing method for the buoy data and from the wave spectrum using Eq. 1 and Eq. 2 for the WAM model data. An investigation carried out on the buoy data set after the records were re-analysed by Fast Fourier Transform to obtain the spectrum, shows that the two definitions produces significantly different results for the mean wave period. On our data set, the mean wave period derived from the zero-up-crossing method compares well with a spectral-derived period based on Eq. 7, although this has been questioned by some authors (see *Goda, 1985, p.37*) However, Eq. 2 was preferred by the WAM development and implementation group (*WAMDI, 1988*) because it is a more stable parameter and a better definition of mean wave period in the context of ocean wave spectral theory. On the buoy data set, the mean wave periods derived from Eq. 2 were found on average 1 to 1.4 sec (20% to 30%) higher than the ones derived from Eq. 7, with a standard deviation of the differences ranging from 0.8 to 1.3 sec. There is thus an urgent need for a common definition to be used. In view of the progresses in wave measurements with the routine availability of observed wave spectra, the same definitions as used by the WAM model (Eq. 1 and Eq. 2) should be agreed upon.

After removal of the discrepancies from the non matching definition discussed in the previous paragraph, the results of the buoy/model comparison are the following. At all buoy locations, the waves are on average 1 m with maximum swh values between 3 m and 5 m, and with short periods, 4-5 sec on average. The model swh analysis and 48-hour forecast are biased low compared to the buoy observations, and the scatter of the differences model minus buoy is rather high, from 30% to 40%. Moreover, the model mean wave period analysis and 48-hour forecast are biased short compared to the buoys observations. Based on both the swh and the mean period comparisons, the WAM model results indicate a less developed sea-state compared to the buoy observations. With slightly higher 48-hour forecast winds, a slightly more developed sea-state is obtained in the 48-hour forecast compared to the analysis.

Because waves are not only locally generated, and because wind observations are scarce and barely at the same location as the wave measurement, it has always been very difficult to distinguish between wind input inaccuracy and inherent wave model inaccuracy in the verification of wave model results. This difficulty is partly overcome by a closer analysis of the results at each buoy locations. The joint use of some new diagrams showing the directional distribution of wind speed and the directional

distribution of significant wave height helps to distinguish between mainly windsea and mainly swell situations.

At Cabopalos, the similarity of the wind and wave directional distribution indicates that the sea-state is mainly windsea dominated. From the integrated parameter comparison (swh and mean wave period, see Table 2 and Table 3), Cabopalos is the location where the model and observation best agree. There is also an impressive agreement between the swh directional distributions (see Fig 6). Compared to the analysis, the 48-hour forecast produces significantly higher northeasterly waves and this is explained by higher 48-hour forecast winds from this direction.

At Capdepera, the comparison of the directional distribution of swh to the directional distribution of wind speed indicates a strong influence of the coast. The discrepancies between the wave model and buoy results are explained by the too coarse resolution of the atmospheric model which does not allow a proper description of the orography of Mallorca and Menorca to obtain the channeling effects between the two islands, by a too coarse resolution of the wave model grid and a too coarse directional discretization of the wave spectra to obtain the proper fetch and propagation around the islands.

At Palamos, the analysis of swh and wind speed distributions indicates an overestimation of the north/northwesterly waves which is attributed to the spatial separation between the buoy and the model nearest grid point. From all the other directions, the waves are underestimated by the model. Many peak swh values are noticeably underestimated by the model. This was found several times during October 1992. Extending the comparison to some neighbouring points, the same peak underestimation is found. This cannot then be attributed to the resolution of the wave model grid which is already finer than the wind model resolution. This underestimation of the peaks has then to be attributed to either a general underestimation of storm peaks by the WAM model, an effect that has already been reported in the Mediterranean Sea by *Guillaume et al. (1992)*, and/or to an underestimation of storm wind speed by the ECMWF T213 atmospheric model as reported by *Cavaleri et al (1991)*.

It is thus expected that a higher resolution in the wave model should improve the results at Capdepera and Cabopalos. However many qualitative aspects of the wind field need to be further quantified in the Mediterranean Sea, such as the accuracy of storm winds, the impact of the atmospheric resolution on the accuracy of coastal winds, the accuracy of forecast winds. From our study storm winds seem to be underestimated by the ECMWF T213 atmospheric model. Coastal effects are partly taken into account at Cabopalos and Palamos, but not enough at Capdepera because the model orography is too coarse to distinguish between the Balearic Islands. The decrease in accuracy found in the 48-hour wave forecast is directly related to the lower accuracy of the 48-hour forecast winds. There seems to be a

systematic overestimation of the wind speed in the 48-hour forecast leading to higher waves with slightly longer period.

References

Cavaleri, L., L. Bertotti, P. Lionello, 1991: Wind wave cast in the Mediterranean Sea. J. Geophys. Res., 96, C6, 10739-10764.

Goda, Y., 1985: Random Seas and Design of Maritime Structures. University of Tokyo Press, 323pp.

Guillaume, A., J.M. Lefèvre, N.M. Mognard, 1992: The use of altimeter data to study the wind and wave variability in the Mediterranean Sea and validate fine-mesh meteorological models. Oceanologica Acta, 15, 5, 555-561.

Juvanon du Vachat R., J.M. Audoin, M. Imbard, L. Musson-Genon and J.P Javelle, 1987: Evaluation of a mesoscale prediction system with surface weather observations and comparison with large-scale prediction system. In Proceeding of the Symposium on Mesoscale Analysis and Forecasting, Vancouver, Canada, 17-19 August 1987, ESA SP-282.

The WAMDI Group: S. and K. Hasselmann, P.A.E.M. Janssen, G.J. Komen, L. Bertotti, P. Lionello, A. Guillaume, V.C. Cardone, J.A. Greenwood, M. Reistad, L. Zambresky, J.A. Ewing, 1988: The WAM model - A third generation ocean wave prediction model. J. Phys. Oceanogr., 18, 1775-1810.

ANNEX A

This annex comprises for each buoy location and on a monthly basis, the time series of the evolution of selected model and buoy parameters for the period October 1992- February 1993.

From top to bottom:

- WAM model significant wave height (solid line) and buoy significant wave height (dots)

- WAM model mean wave period (solid line) and buoy mean wave period (dots)

- WAM model mean wave direction

- T213 ECMWF 10m wind speed

- T213 ECMWF 10m wind direction

- T213 ECMWF 2m temperature

For the significant wave height and mean wave period, the results of the monthly statistical comparison are given in the right margin:
M-MEA, mean of the model values, O-MEA, mean of the buoy values,
M-STD, standard deviation of the model values, O-STD, standard deviation of the buoy values,
ERSTD, mean difference (or bias), i.e. mean of the differences model minus buoy values,
SCATI, scatter index,
SLOPE (resp. INTER), slope (resp. intercept) of the linear regression.

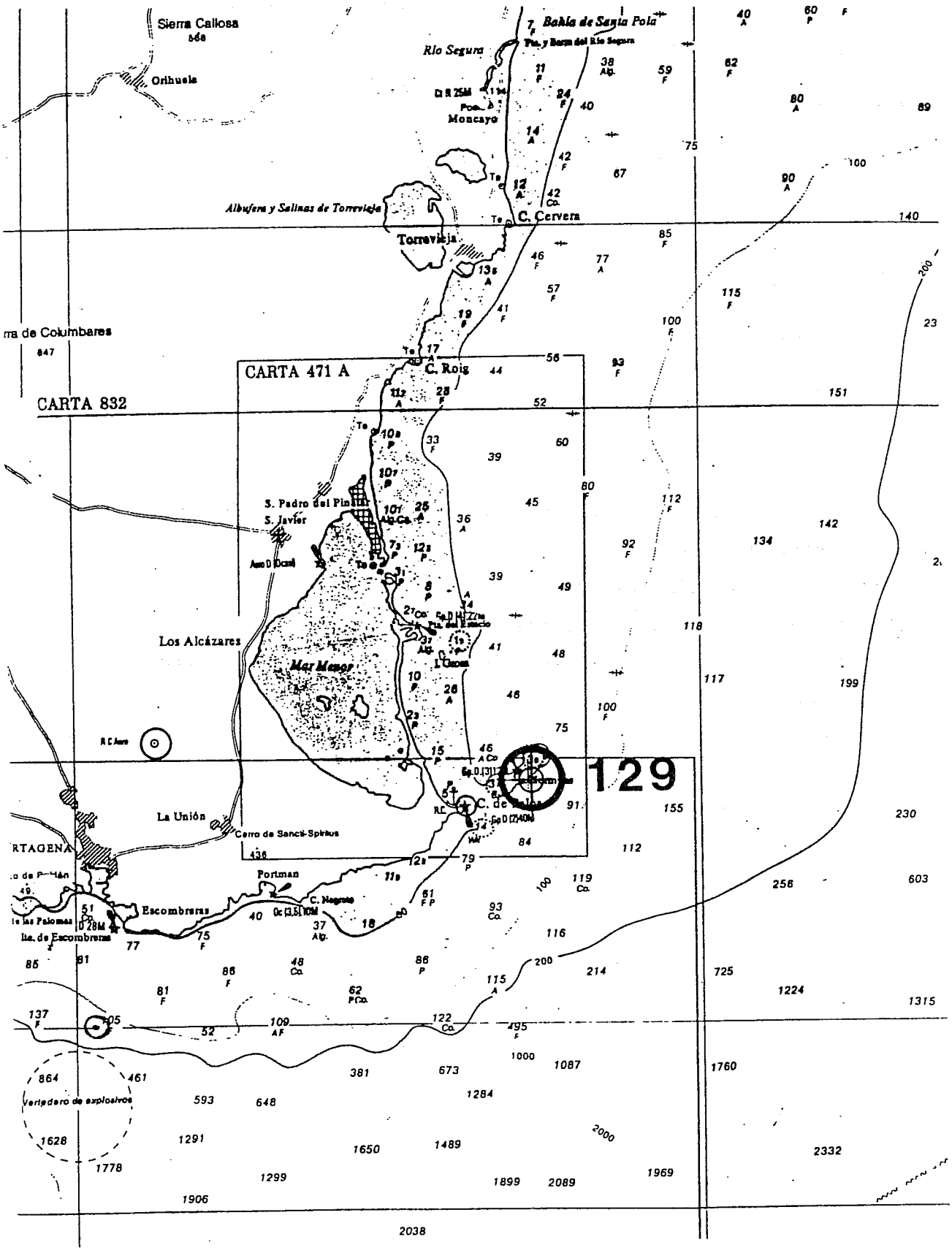
Sierra Callosa
568
Orihuela
Río Segura
Bahía de Santa Pola
Pta. y Barra del Río Segura
Moncayo
Albufera y Salinas de Torrevieja
C. Cervera
Torrevieja
ma de Columbares
847
CARTA 471 A
C. Roig
CARTA 832
S. Pedro del Pinatar
S. Javier
Los Alcázares
Mar Menor
La Unión
Cerro de Sancti-Spiritus
RTAGENA
Portman
C. Negrete
Escombreras
lla. de Escombreras
Vertedero de explosivos
129

BOYA DE CABOPALO

Numero de Codigo : 129

Coordenadas Geograficas

Longitud : 0 gr. 37' 48'' O

Latitud : 37 gr. 39' 00'' N

Profundidad : 67 metros

Procedencia : R.E.M.R.O.

Tipo de boya : Escalar (Waverider Datawell)

Tipo de datos : Procesados y registros brutos

Estado actual : En funcionamiento

ANALYSIS

CABOPAL (37.7N -0.6E)
OCTOBER 1992

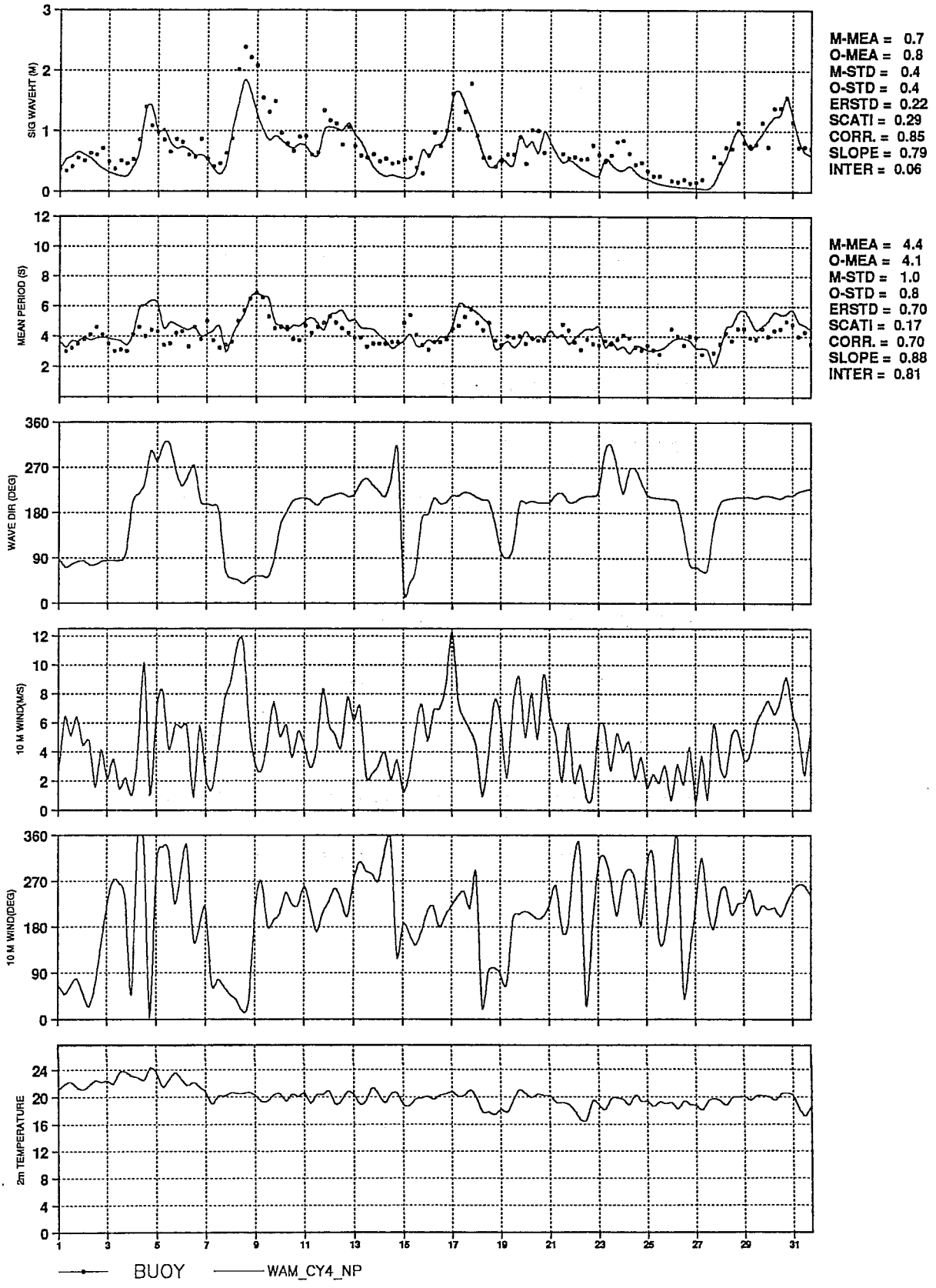

48-hours FORECAST

CABOPAL (37.7N -0.6E)
OCTOBER 1992

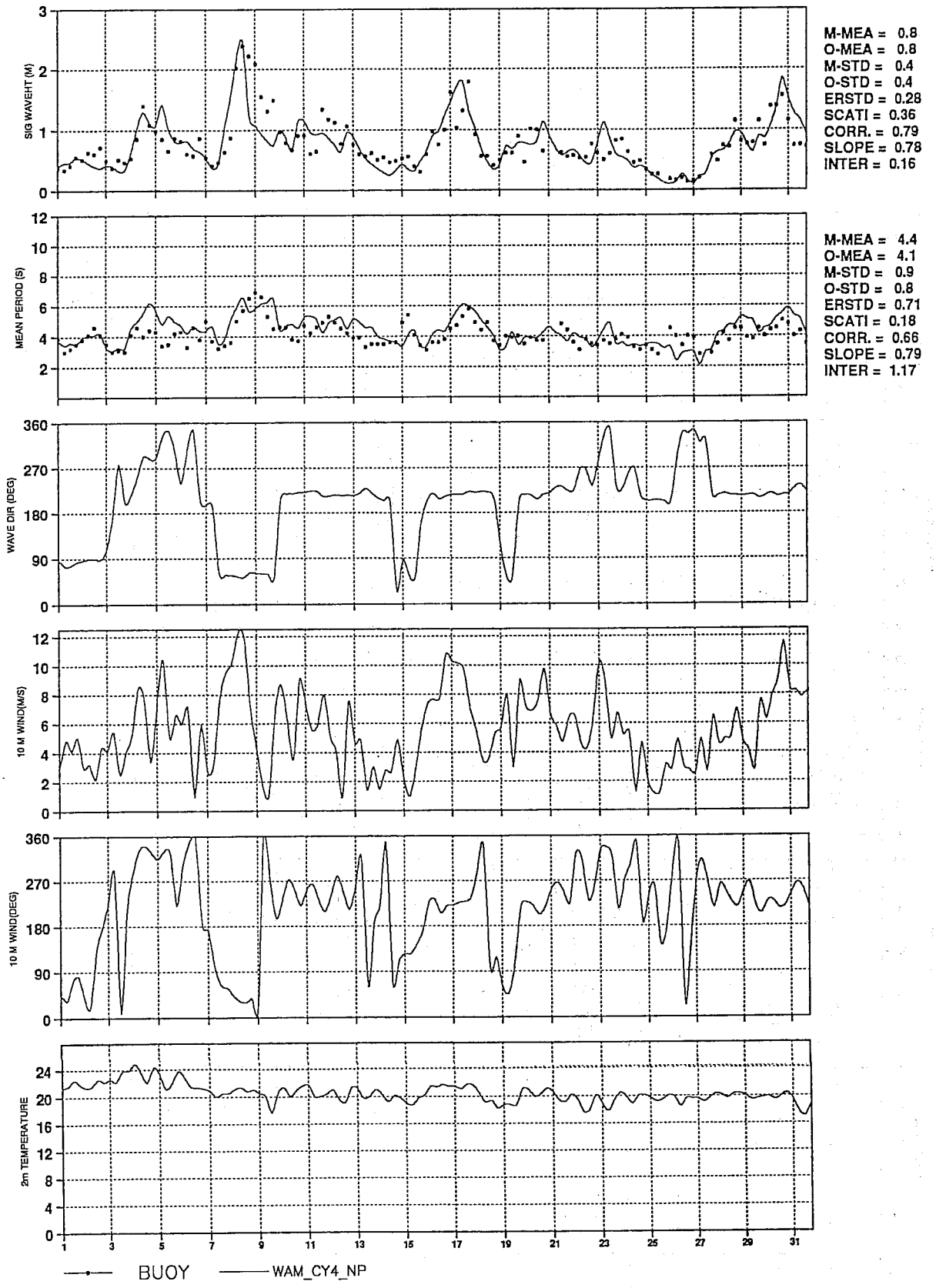

ANALYSIS

CABOPAL (37.7N -0.6E)
NOVEMBER 1992

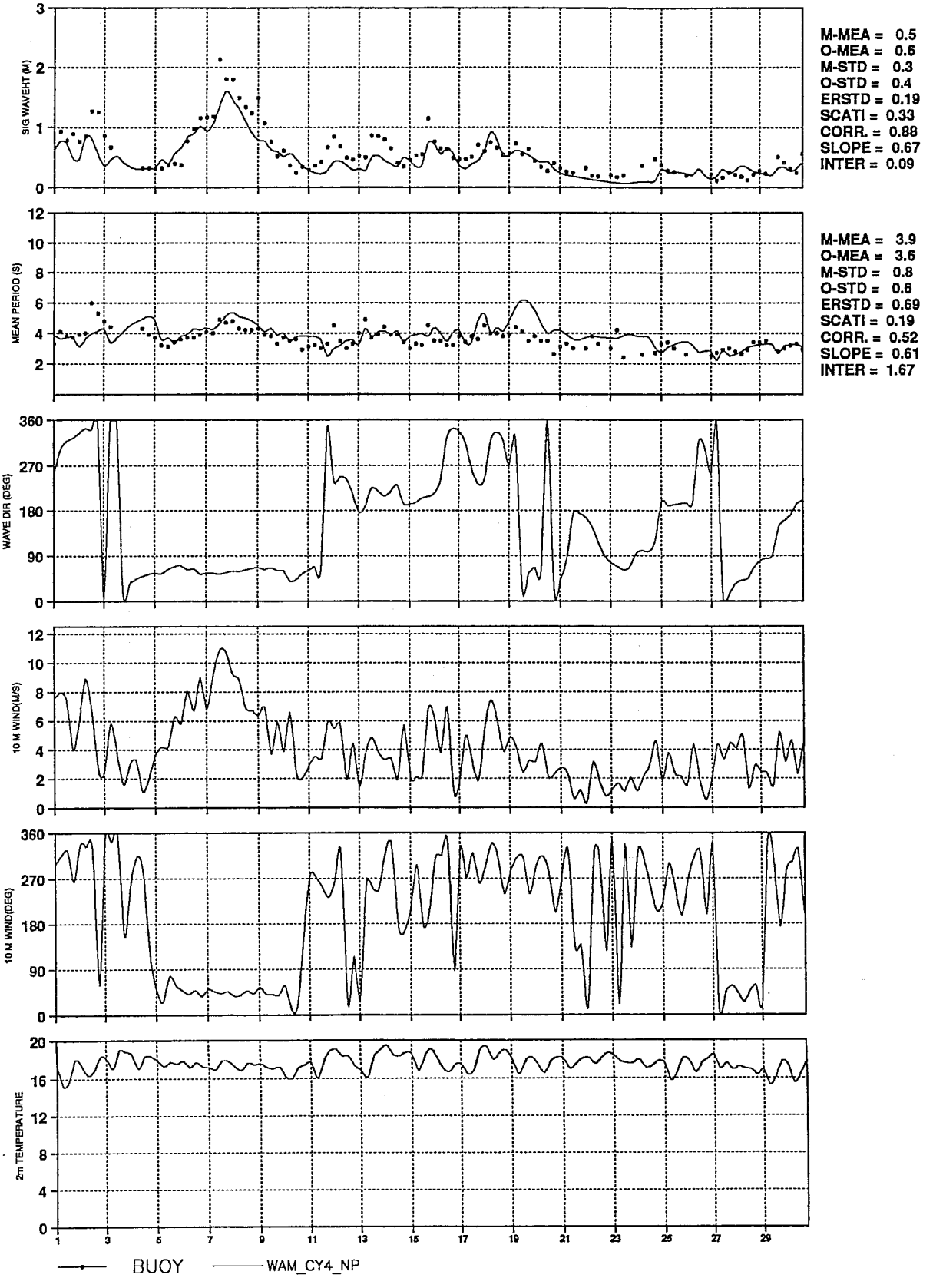

48-hours FORECAST

CABOPAL (37.7N -0.6E)
NOVEMBER 1992

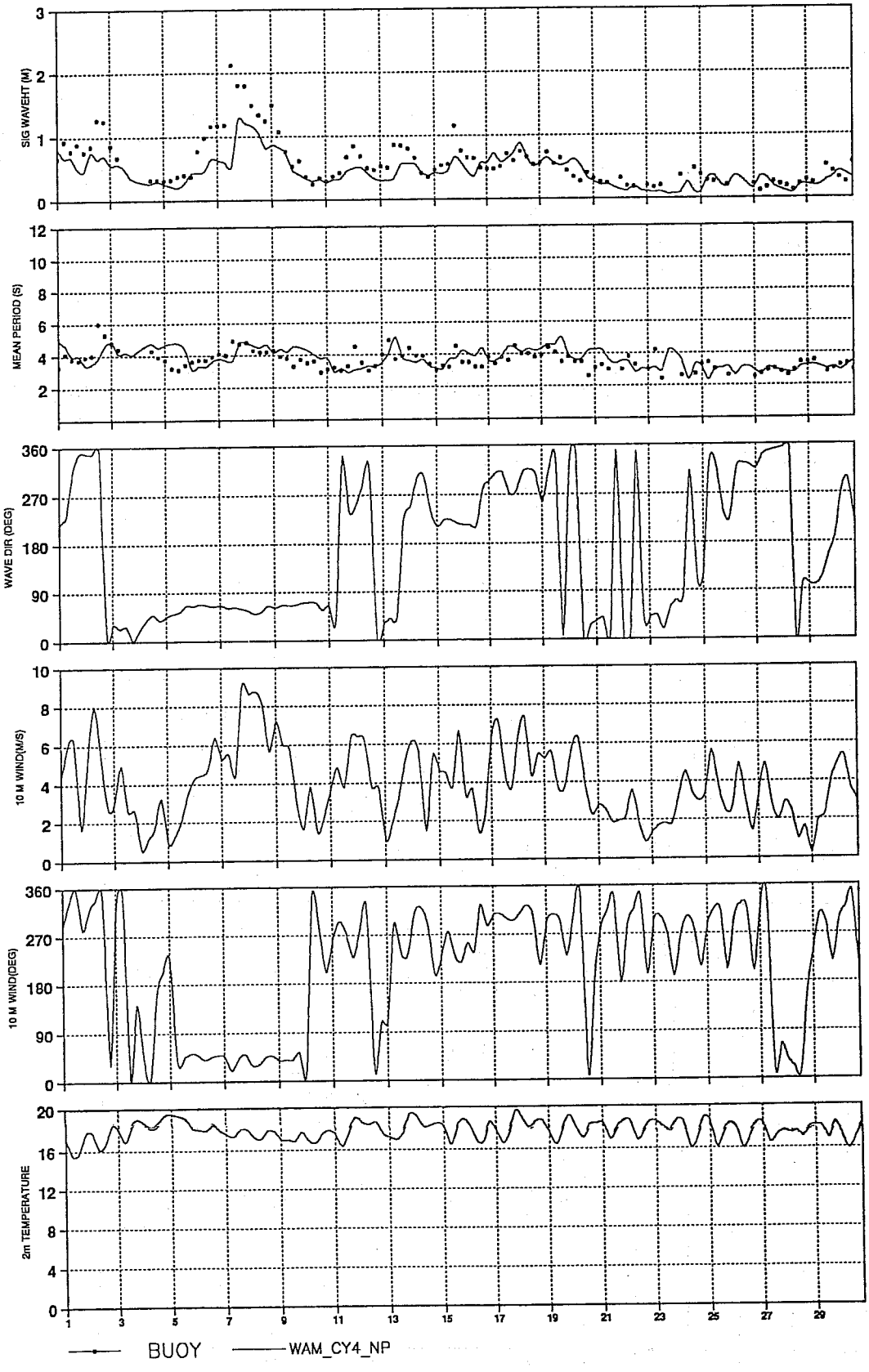

ANALYSIS

CABOPAL (37.7N -0.6E)
DECEMBER 1992

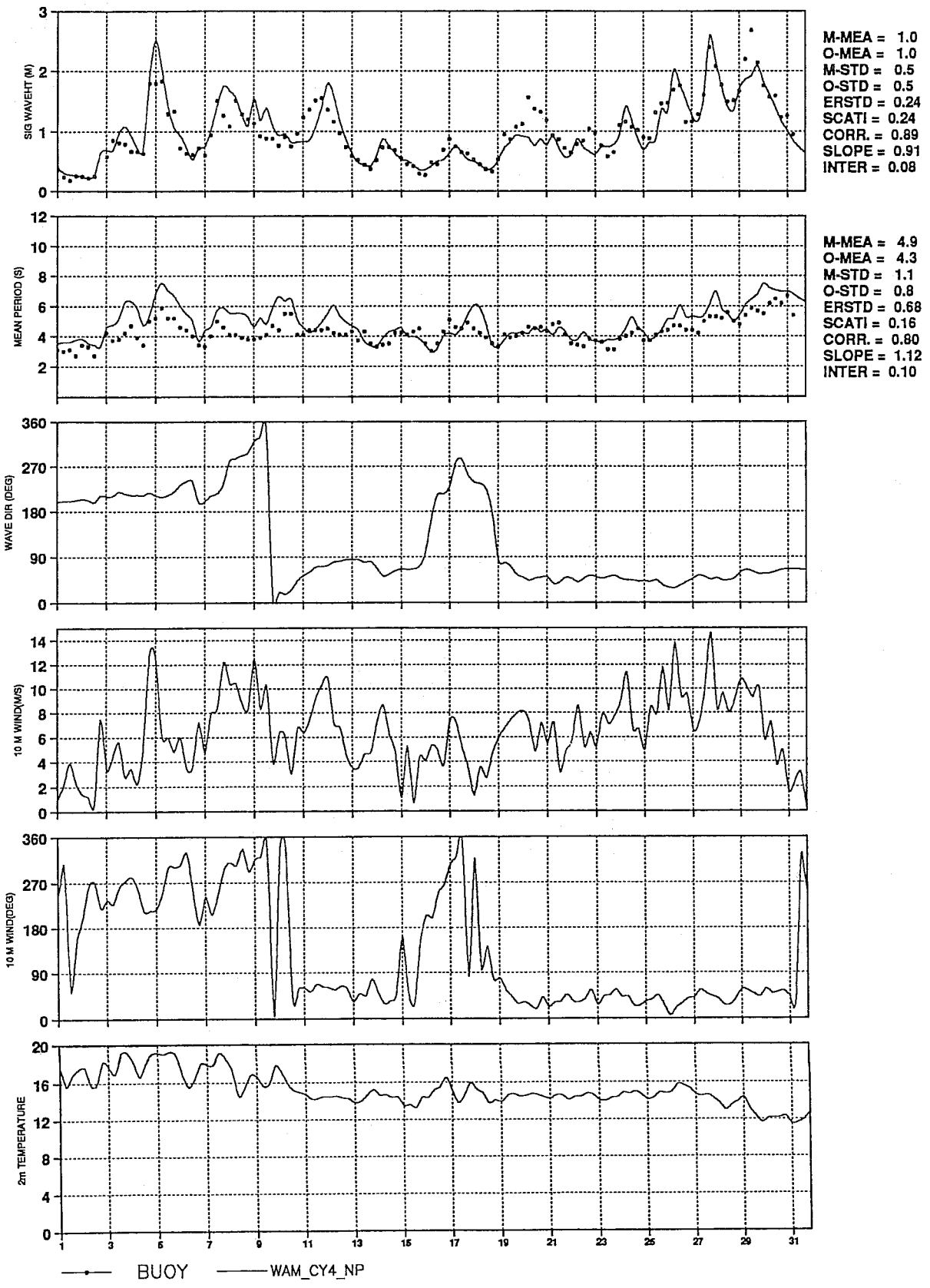

48-hours FORECAST

CABOPAL (37.7N -0.6E)
DECEMBER 1992

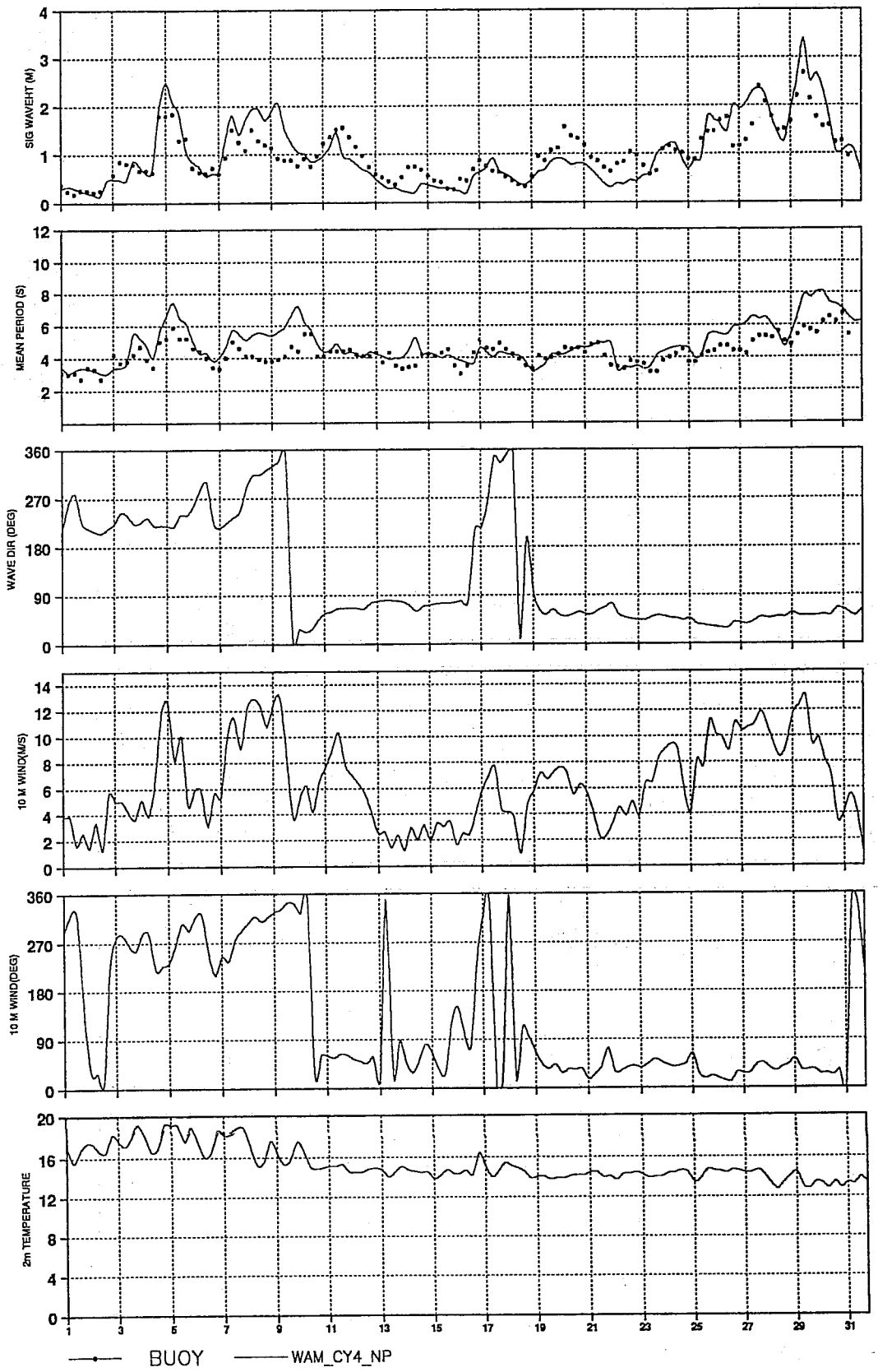

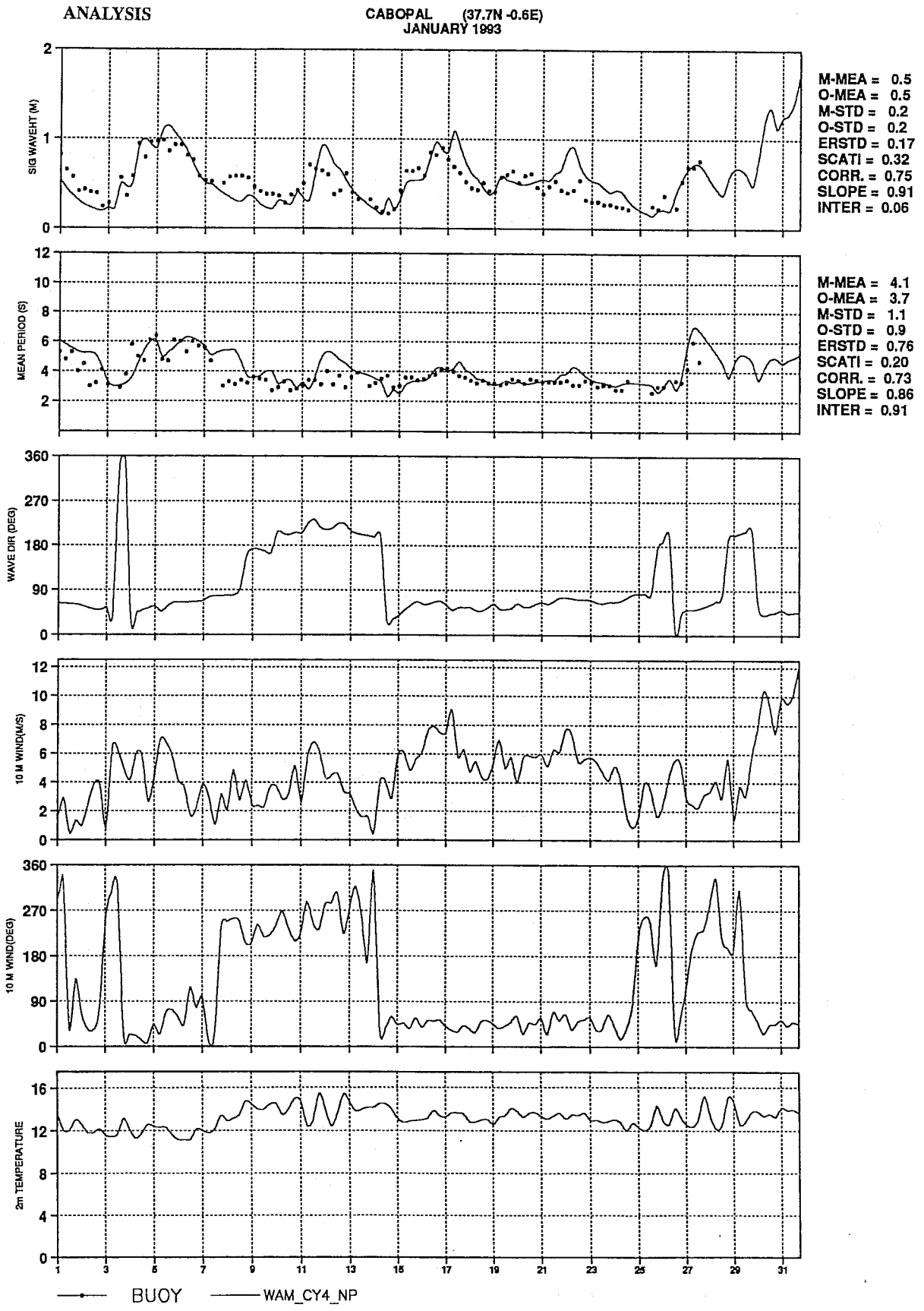
ANALYSIS
CABOPAL (37.7N -0.6E)
JANUARY 1993
SIG WAVEHT (M)
M-MEA = 0.5
O-MEA = 0.5
M-STD = 0.2
O-STD = 0.2
ERSTD = 0.17
SCATI = 0.32
CORR. = 0.75
SLOPE = 0.91
INTER = 0.06
MEAN PERIOD (S)
M-MEA = 4.1
O-MEA = 3.7
M-STD = 1.1
O-STD = 0.9
ERSTD = 0.76
SCATI = 0.20
CORR. = 0.73
SLOPE = 0.86
INTER = 0.91
WAVE DIR (DEG)
10 M WIND(M/S)
10 M WIND(DEG)
2m TEMPERATURE
BUOY
WAM_CY4_NP

48-hours FORECAST

CABOPAL (37.7N -0.6E)
JANUARY 1993

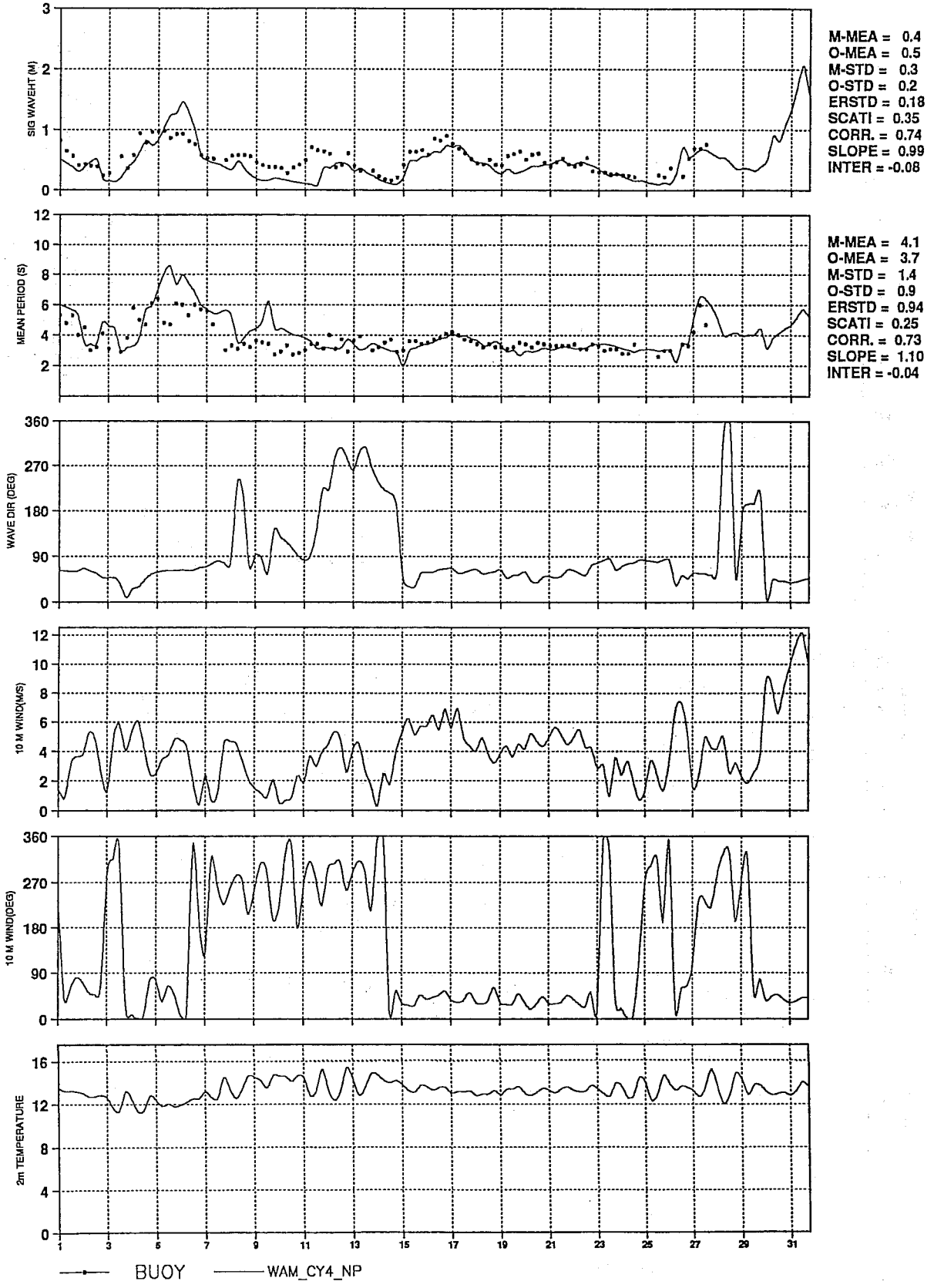

ANALYSIS

CABOPAL (37.7N -0.6E)
FEBRUARY 1993

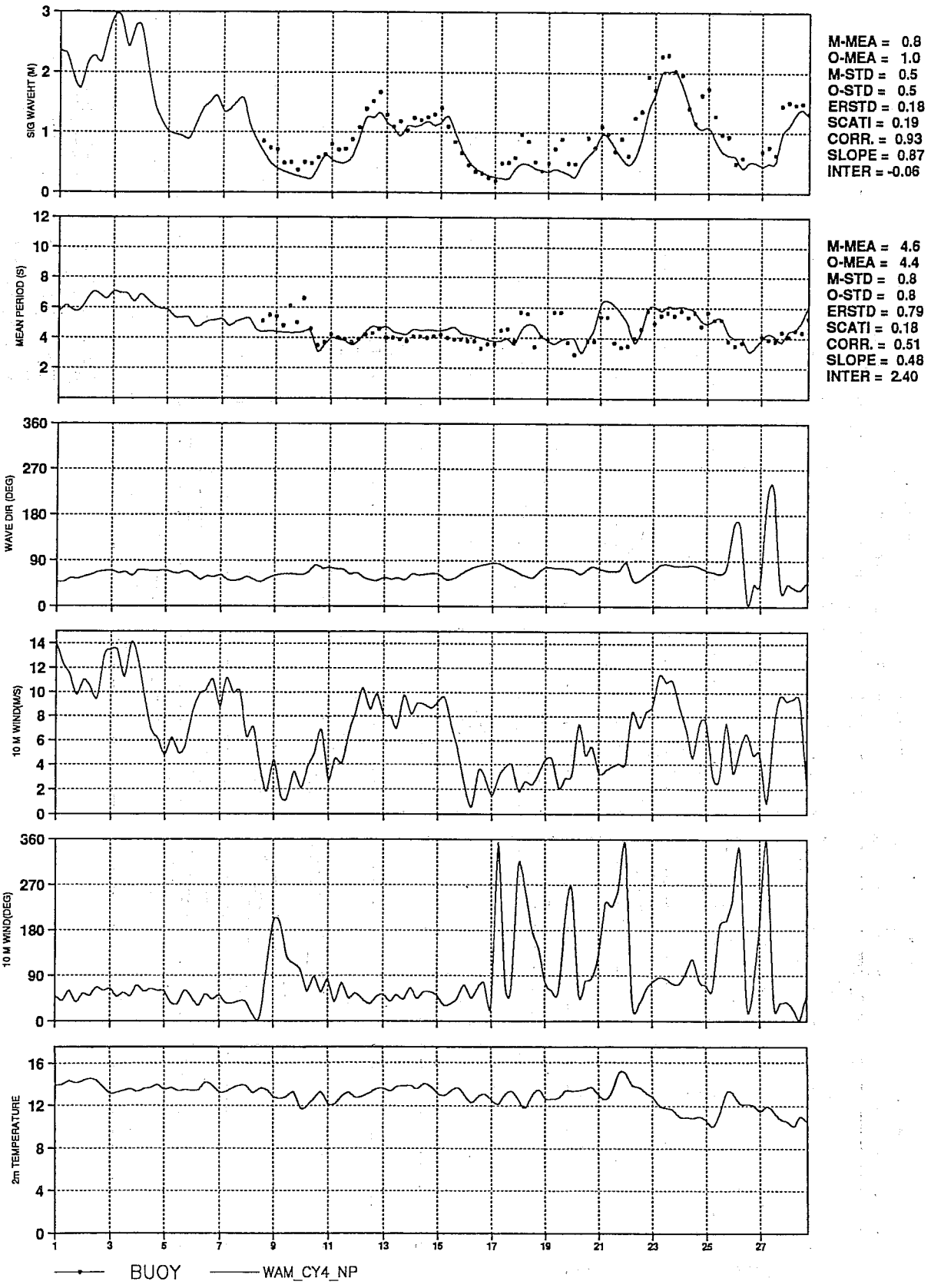

48-hours FORECAST

CABOPAL (37.7N -0.6E)
FEBRUARY 1993

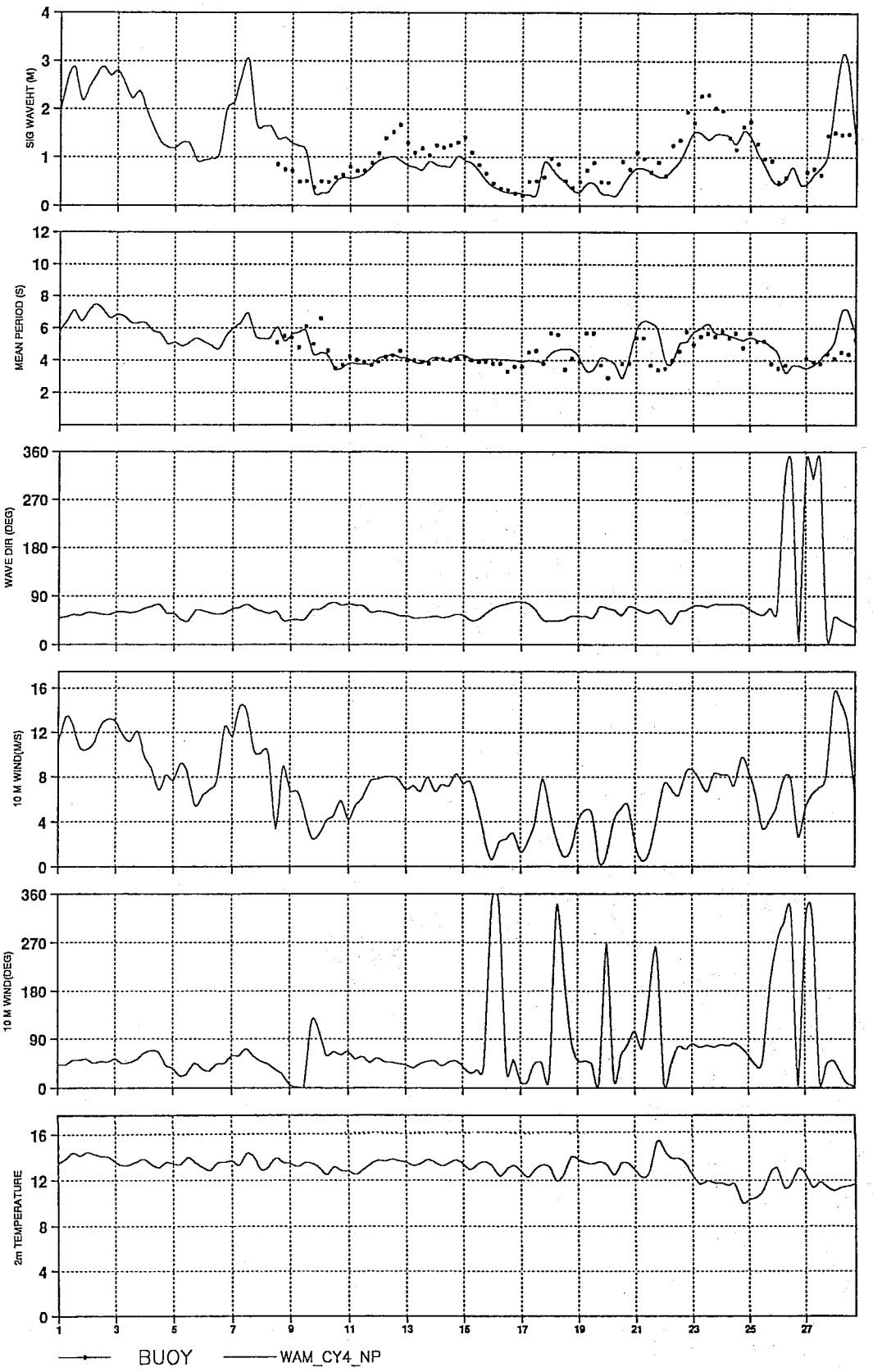

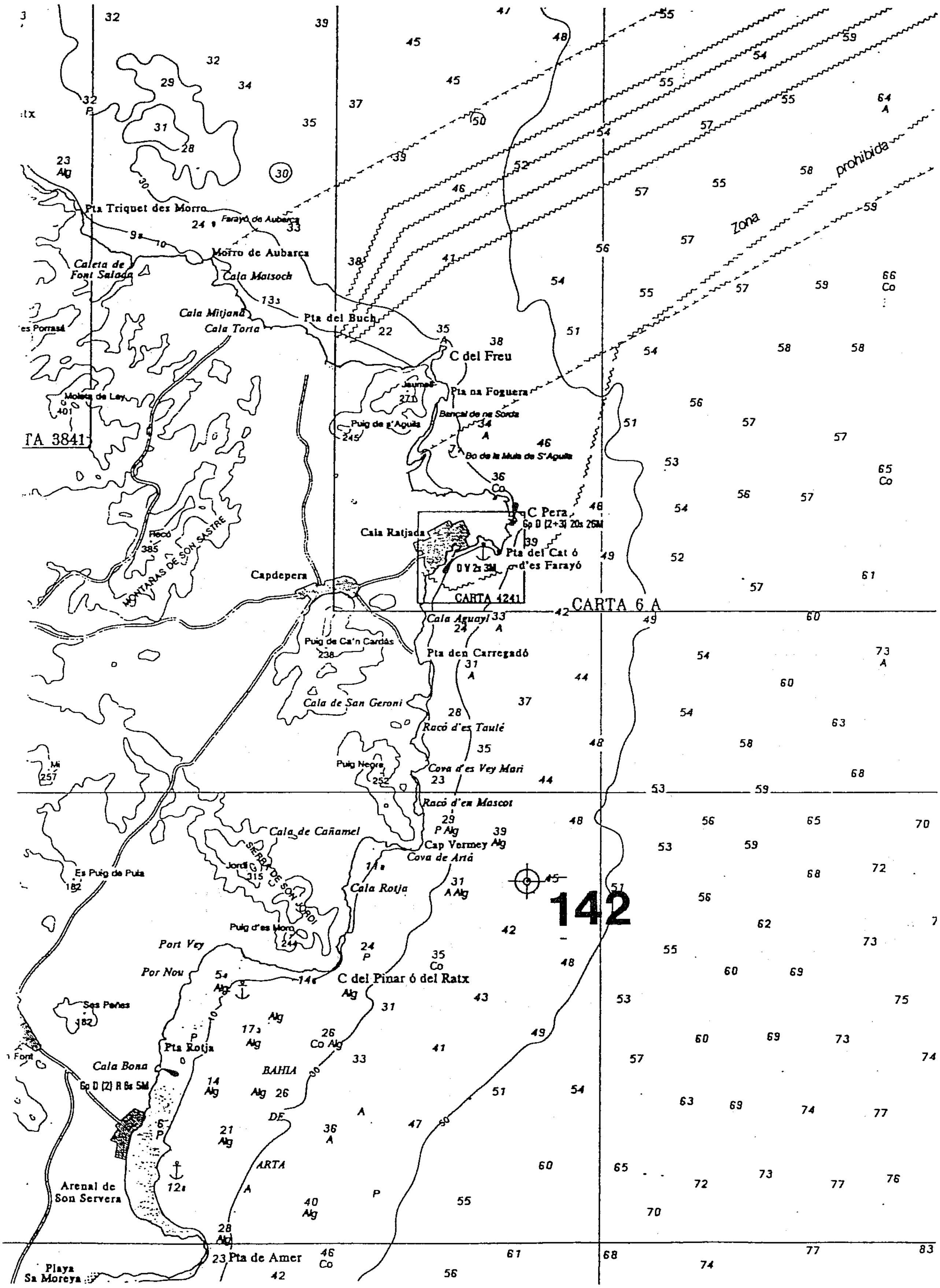
Pta Triquet des Morro
Farayó de Aubarca
Morro de Aubarca
Caleta de Font Salada
Cala Matsoch
Cala Mitjana
Cala Torta
Pta del Buch
C del Freu
Pta na Foguera
Puig de s'Aguila
Bancal de na Sorda
Bo de la Mula de S'Aguila
Molets de Ley
TA 3841
C Pera
Gp D (2+3) 20s 26M
Cala Ratjada
Pta del Cat ó d'es Farayó
D V 2s 3M
CARTA 4241
CARTA 6 A
Capdepera
MONTAÑAS DE SON SASTRE
Recó
Zona prohibida
Cala Aguayl
Puig de Ca'n Cardás
Pta den Carregadó
Cala de San Geroni
Racó d'es Taulé
Puig Negre
Cova d'es Vey Marí
Racó d'en Mascot
Cala de Cañamel
Cap Vermey
Cova de Artá
SIERRA DE SON JORDI
Es Puig de Pula
Cala Rotja
Puig d'es Moro
142
Port Vey
Por Nou
C del Pinar ó del Ratx
Ses Peñes
Pta Rotja
Cala Bona
Gp D (2) R 6s 5M
BAHIA DE ARTA
Arenal de Son Servera
Pta de Amer
Playa Sa Moreya

BOYA DE CAPDEPER

Numero de Codigo : 142

Coordenadas Geograficas

Longitud : 3 gr. 29' 07'' E

Latitud : 39 gr. 39' 04'' N

Profundidad : 48 metros

Procedencia : R.E.M.R.O.

Tipo de boya : Escalar (Waverider Datawell)

Tipo de datos : Procesados y registros brutos

Estado actual : En funcionamiento

ANALYSIS

CAPDEP (39.7N 3.5E)
OCTOBER 1992

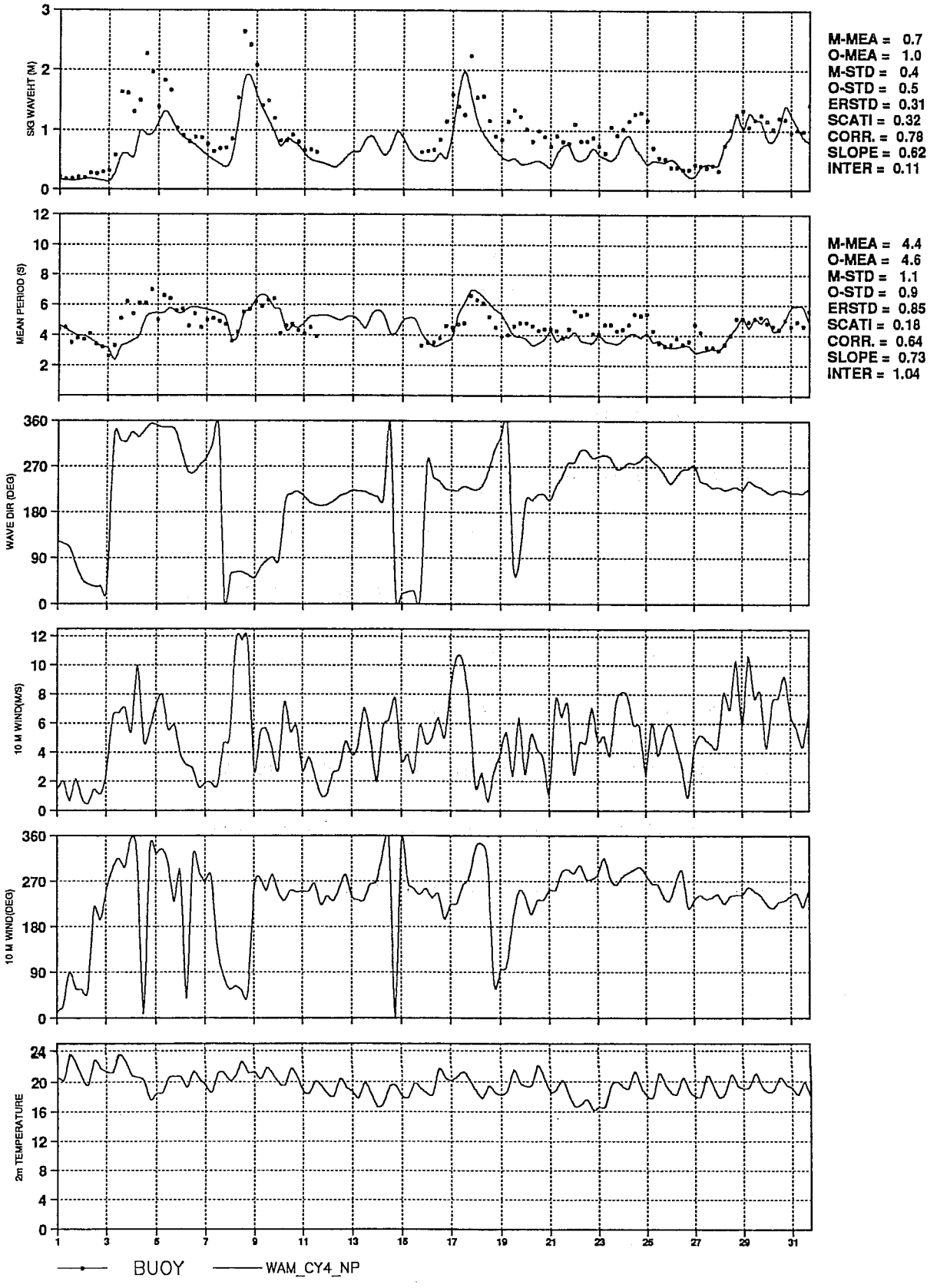

48-hours FORECAST

CAPDEP (39.7N 3.5E)
OCTOBER 1992

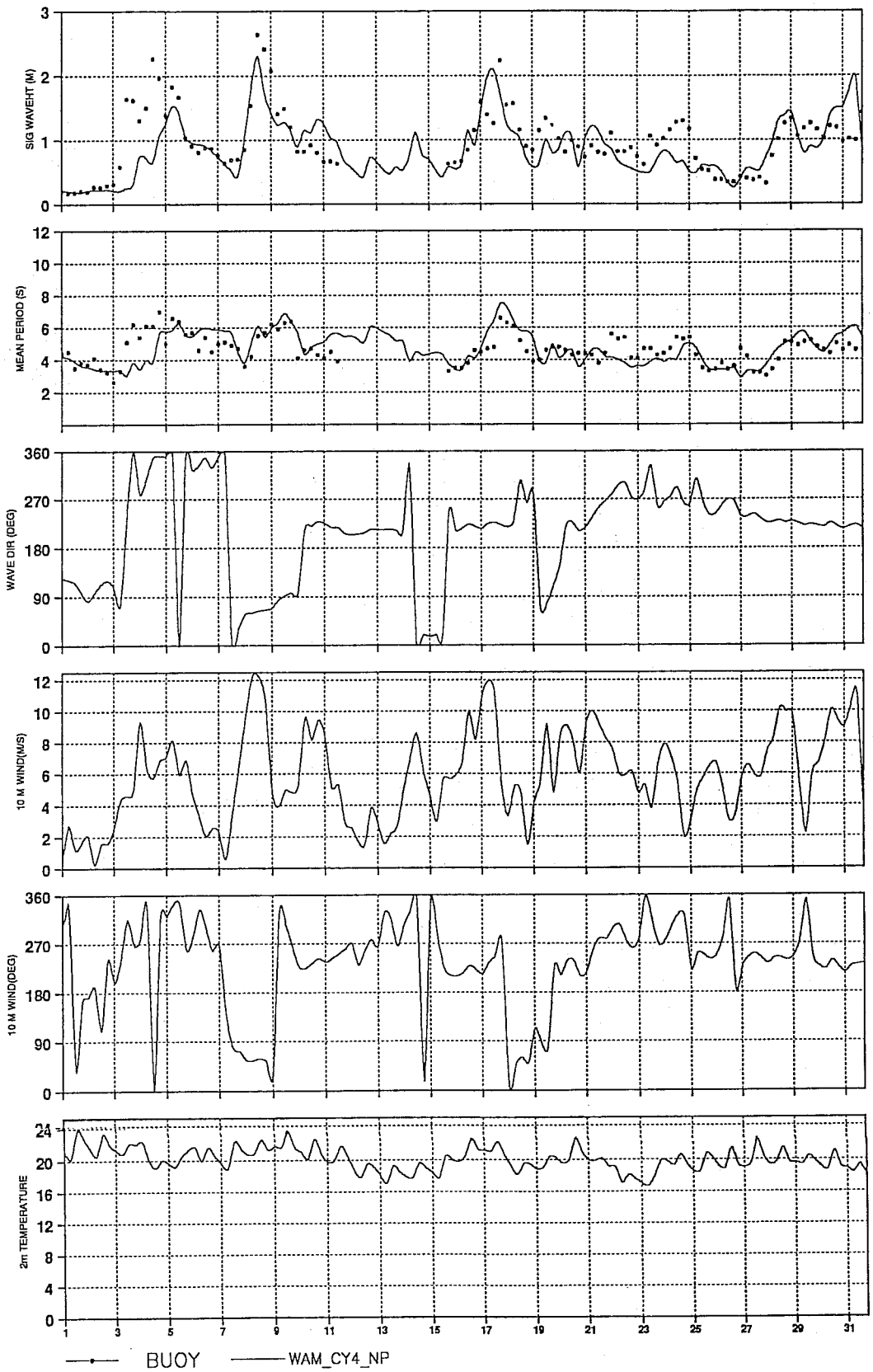

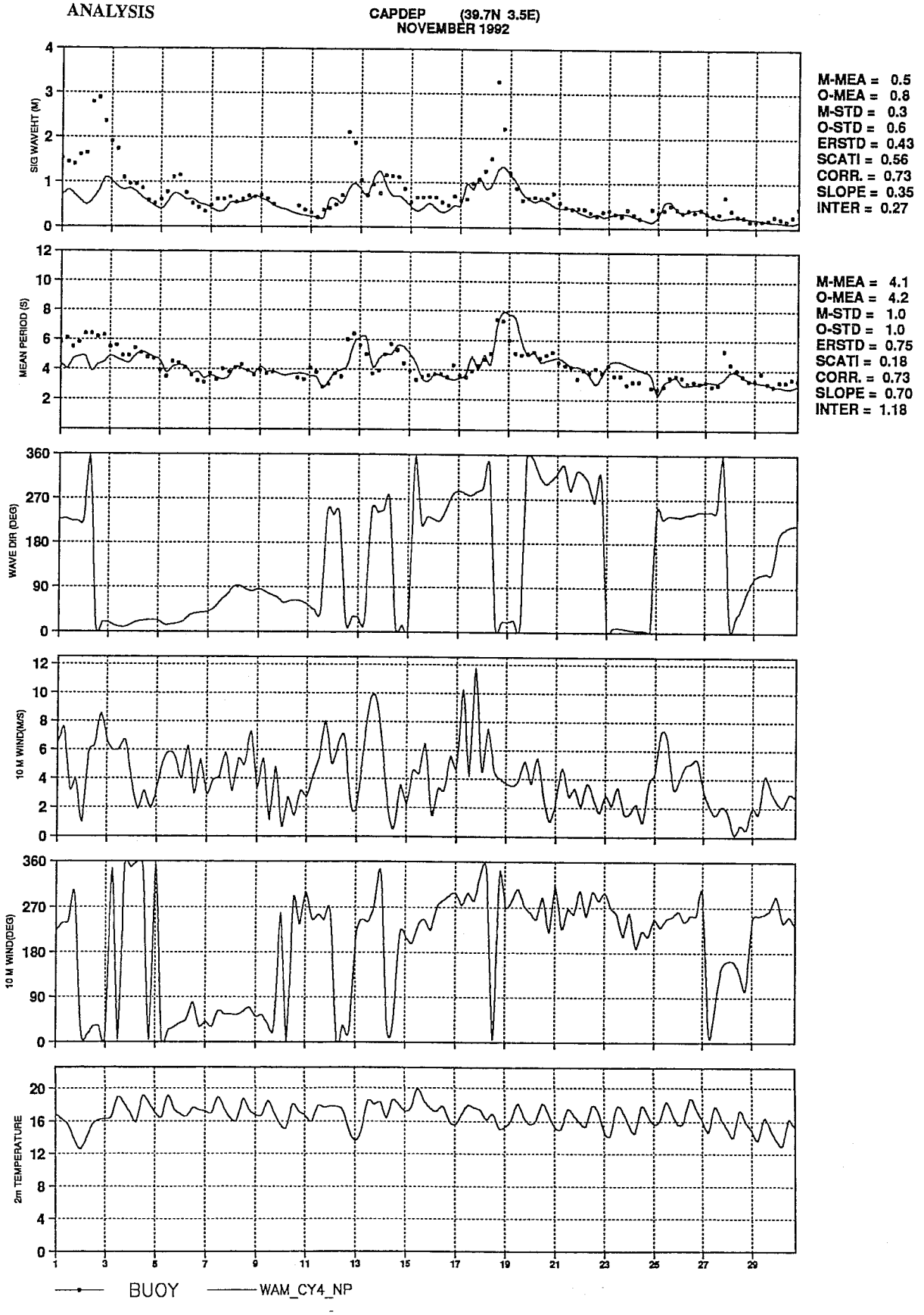
ANALYSIS
CAPDEP (39.7N 3.5E)
NOVEMBER 1992
SIG WAVEHT (M)
M-MEA = 0.5
O-MEA = 0.8
M-STD = 0.3
O-STD = 0.6
ERSTD = 0.43
SCATI = 0.56
CORR. = 0.73
SLOPE = 0.35
INTER = 0.27
MEAN PERIOD (S)
M-MEA = 4.1
O-MEA = 4.2
M-STD = 1.0
O-STD = 1.0
ERSTD = 0.75
SCATI = 0.18
CORR. = 0.73
SLOPE = 0.70
INTER = 1.18
WAVE DIR (DEG)
10 M WIND(M/S)
10 M WIND(DEG)
2m TEMPERATURE
BUOY
WAM_CY4_NP

48-hours FORECAST

CAPDEP (39.7N 3.5E)
NOVEMBER 1992

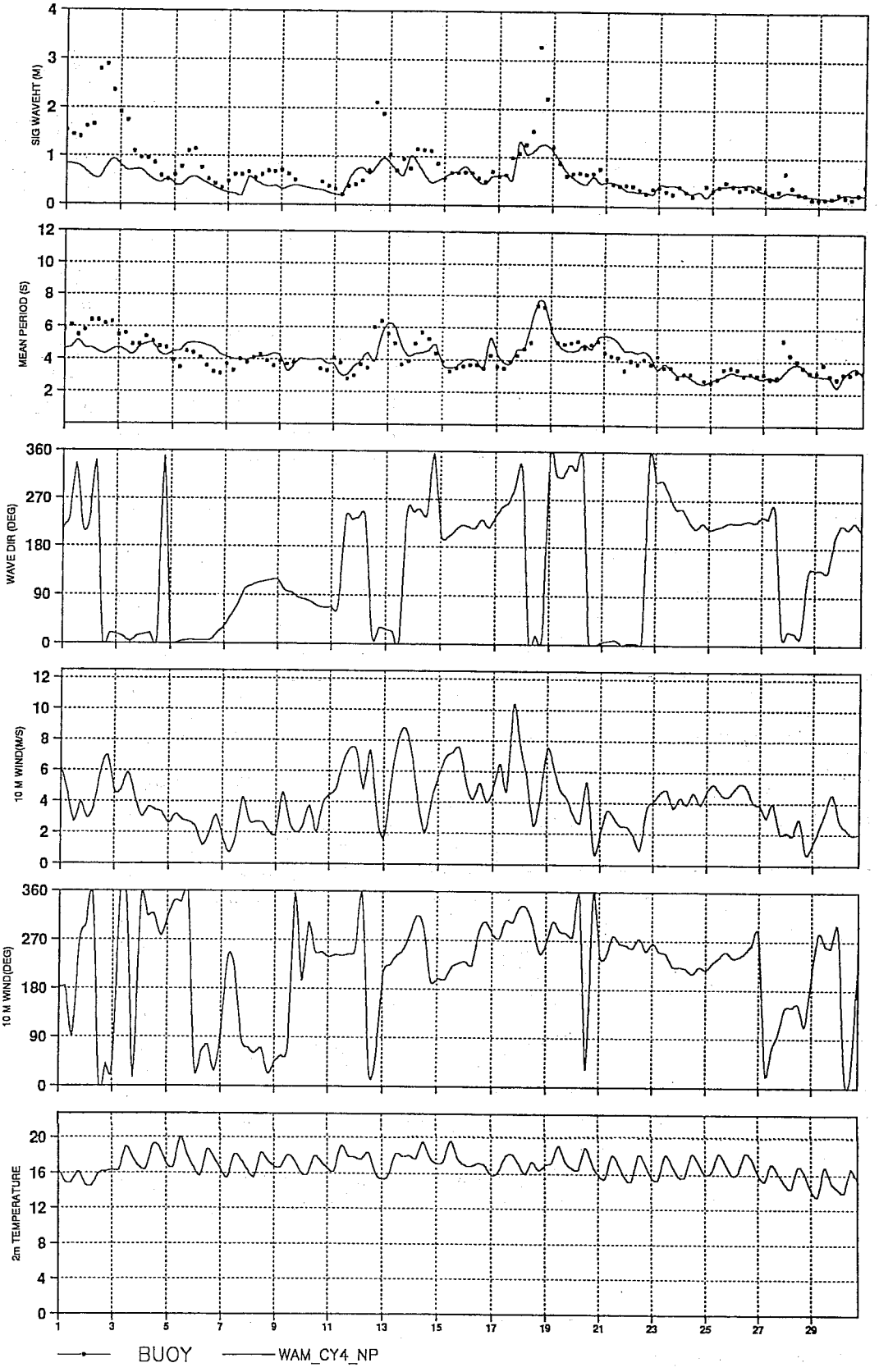

ANALYSIS

CAPDEP (39.7N 3.5E)
DECEMBER 1992

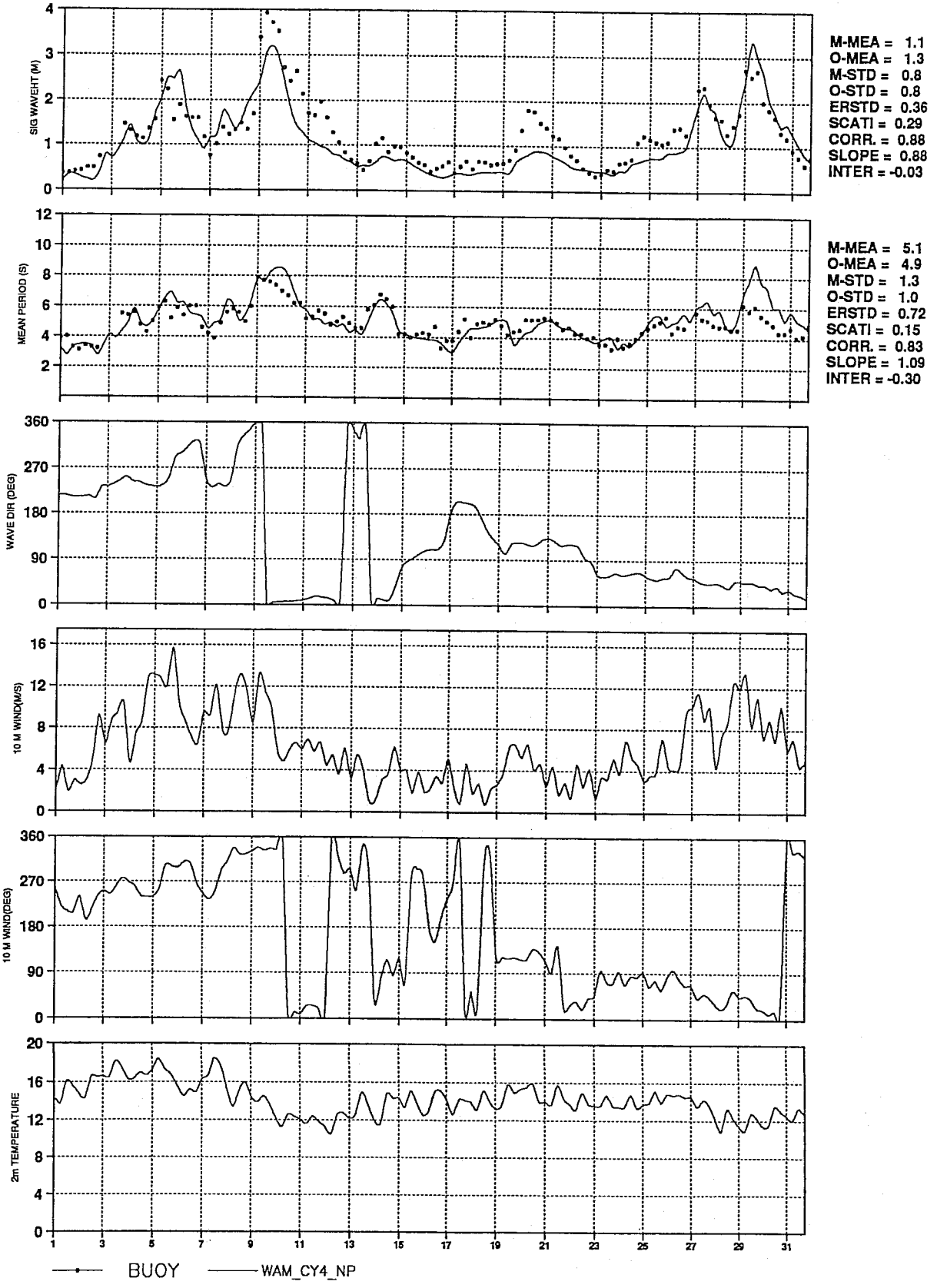

48-hours FORECAST

CAPDEP (39.7N 3.5E)
DECEMBER 1992

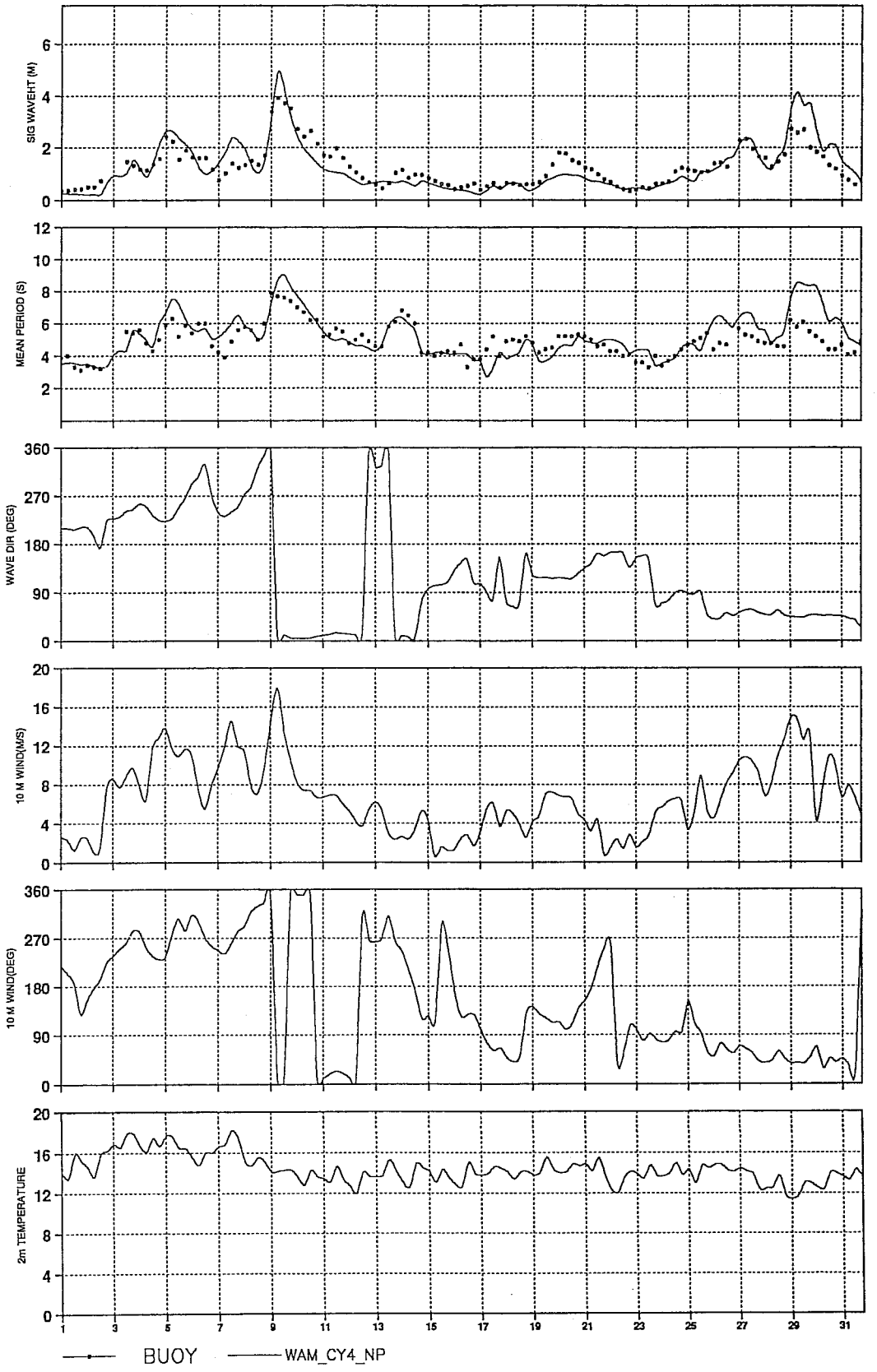

ANALYSIS

CAPDEP (39.7N 3.5E)
JANUARY 1993

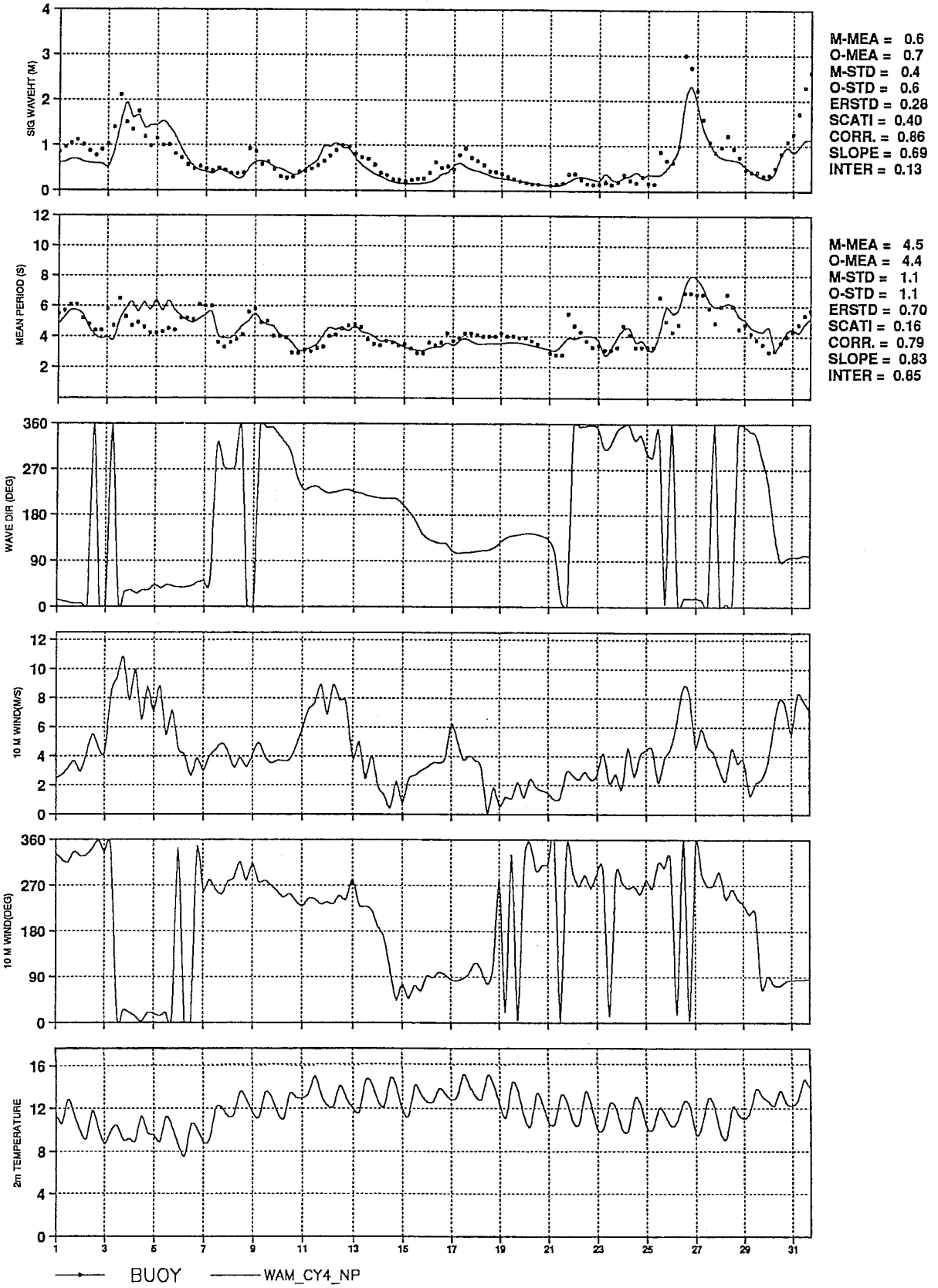

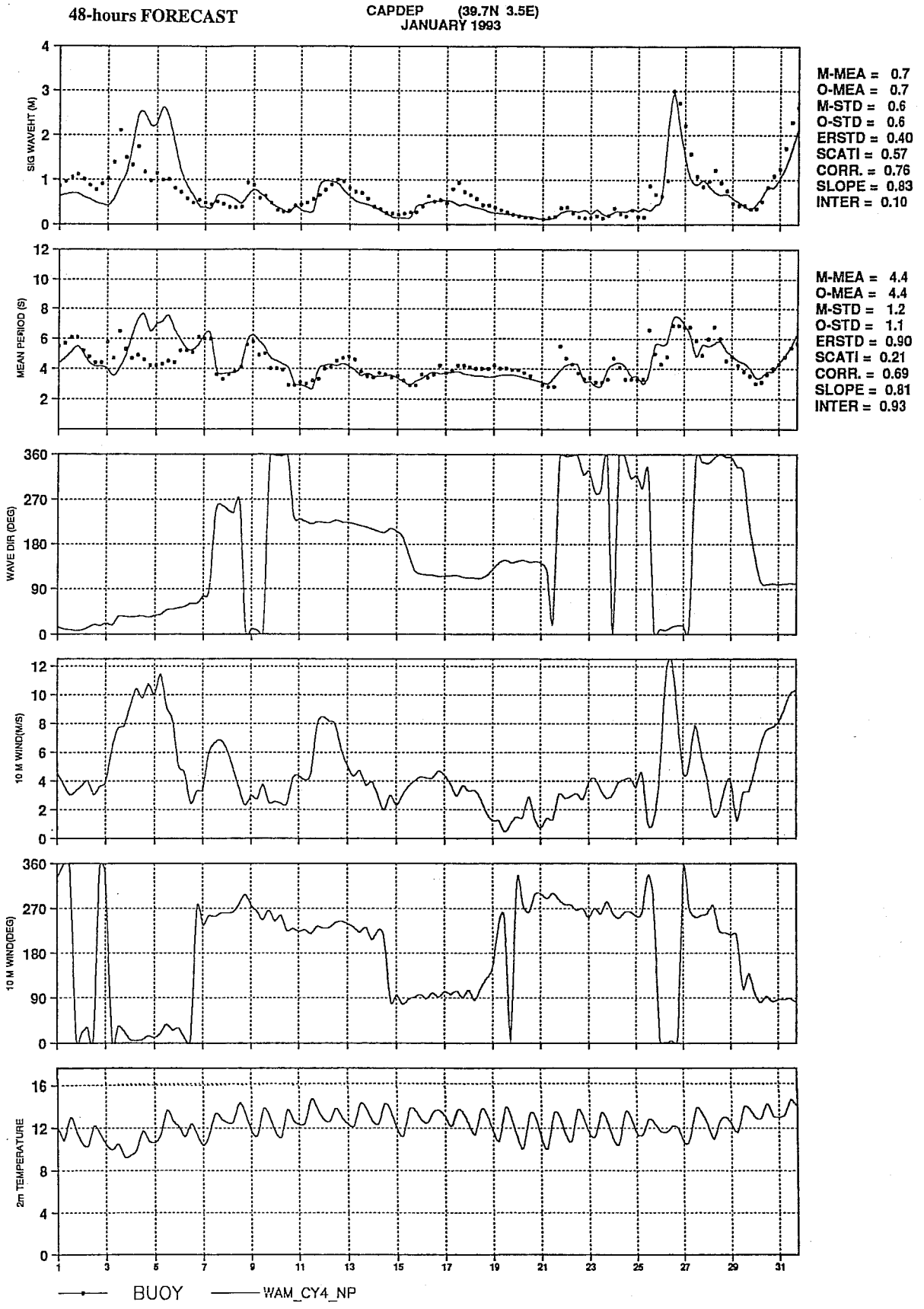
48-hours FORECAST
CAPDEP (39.7N 3.5E)
JANUARY 1993
SIG WAVEHT (M)
M-MEA = 0.7
O-MEA = 0.7
M-STD = 0.6
O-STD = 0.6
ERSTD = 0.40
SCATI = 0.57
CORR. = 0.76
SLOPE = 0.83
INTER = 0.10
MEAN PERIOD (S)
M-MEA = 4.4
O-MEA = 4.4
M-STD = 1.2
O-STD = 1.1
ERSTD = 0.90
SCATI = 0.21
CORR. = 0.69
SLOPE = 0.81
INTER = 0.93
WAVE DIR (DEG)
10 M WIND(M/S)
10 M WIND(DEG)
2m TEMPERATURE
BUOY
WAM_CY4_NP

ANALYSIS

CAPDEP (39.7N 3.5E)
FEBRUARY 1993

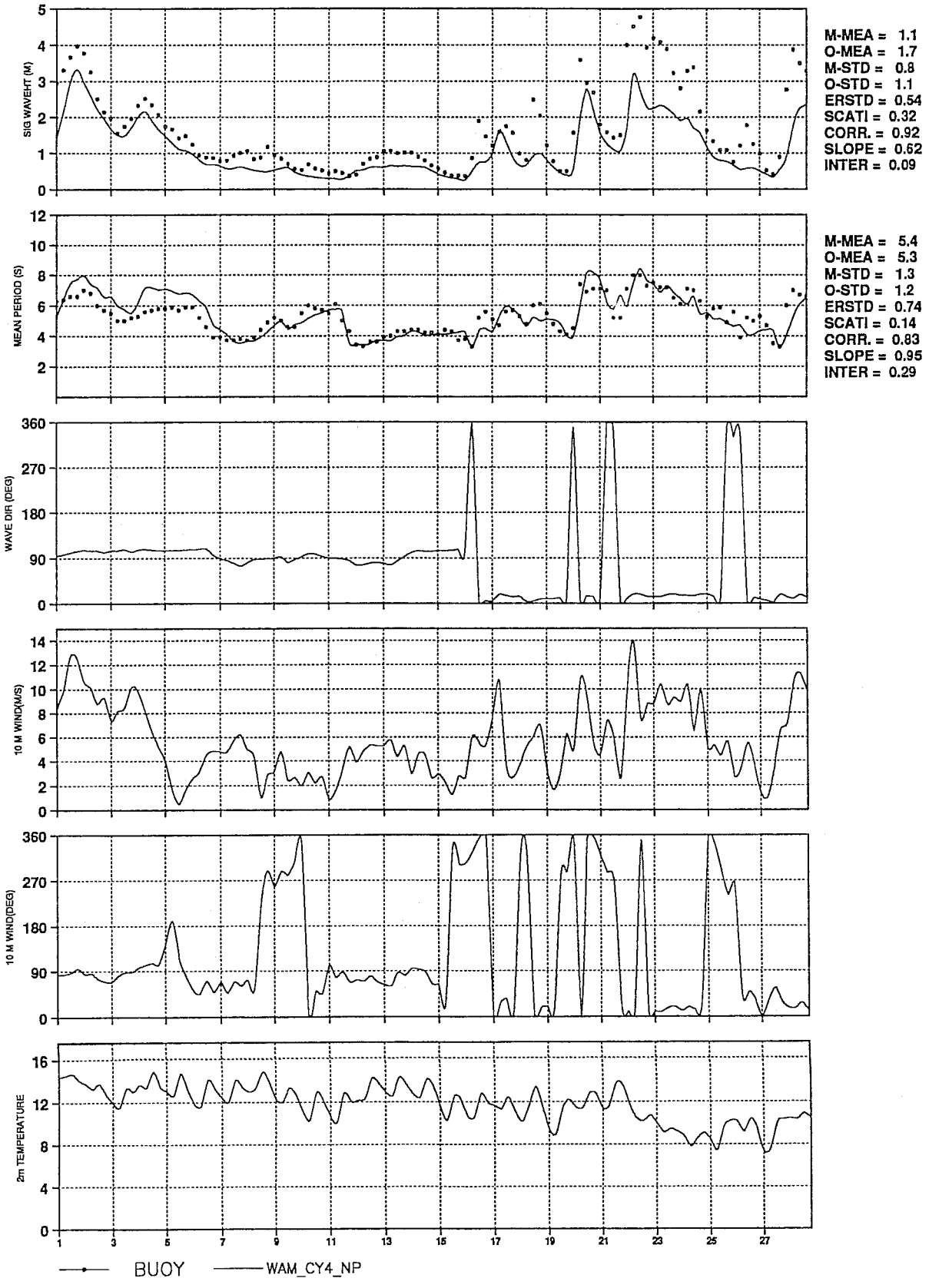

48-hours FORECAST

CAPDEP (39.7N 3.5E)
FEBRUARY 1993

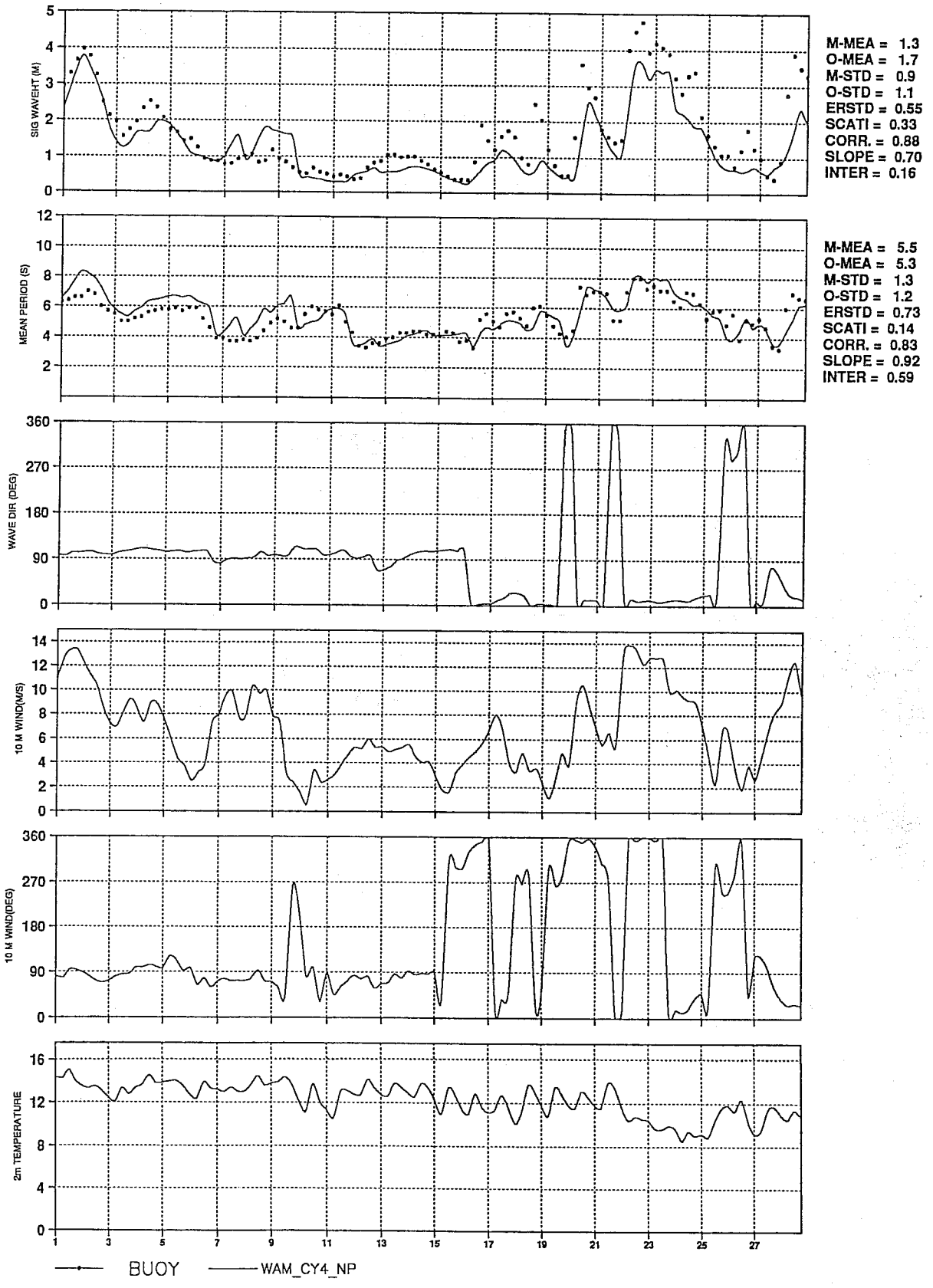

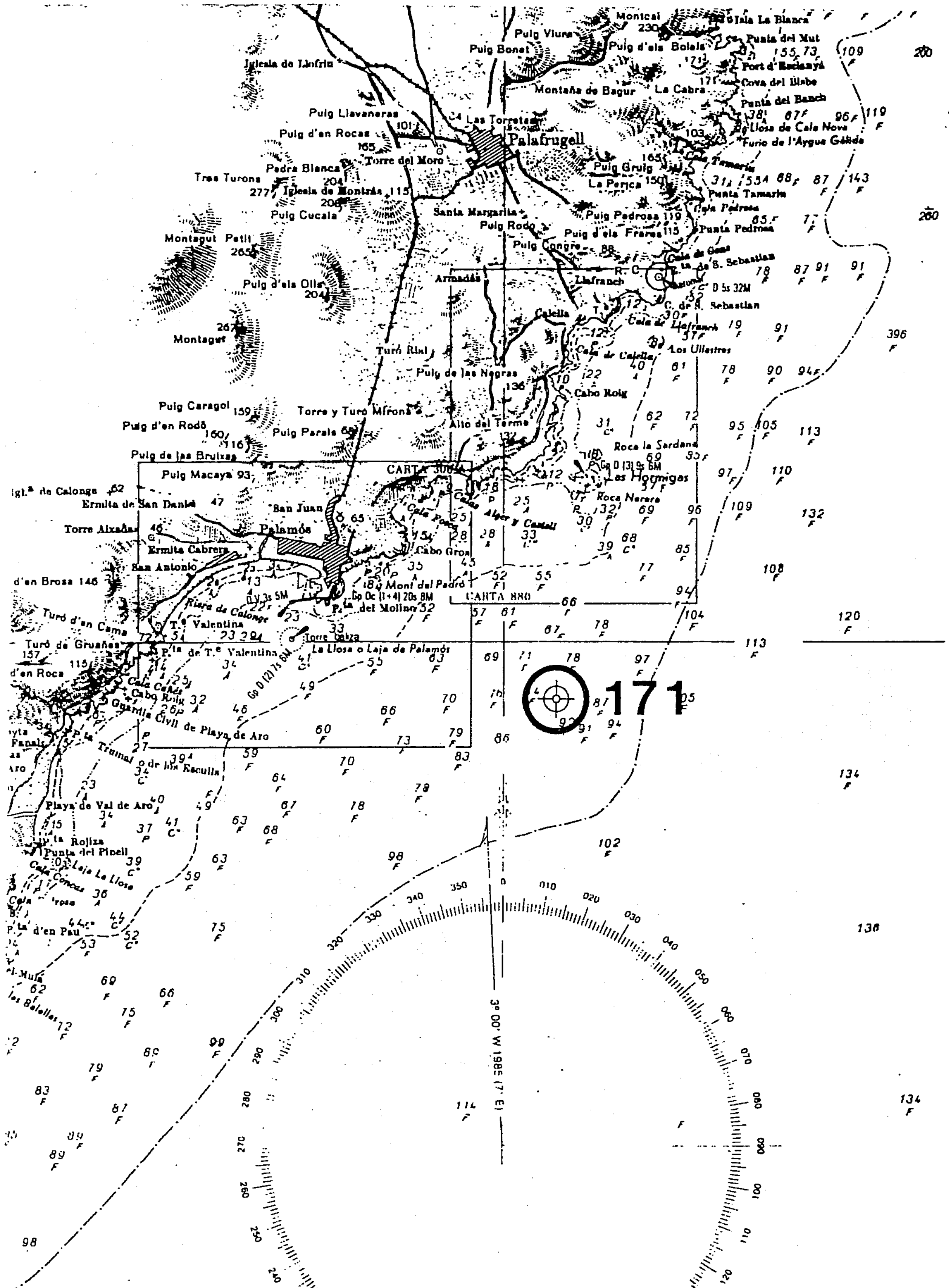

Montcal
Isla La Blanca
Puig Viura
Punta del Mut
Puig Bonet
Puig d'els Bolels
Port d'Esclanyá
Iglesia de Llofriu
Cova del Bisbe
Montaña de Bagur
La Cabra
Punta del Banch
Puig Llavaneras
Las Torretas
Llosa de Cala Nova
Puig d'en Rocas
Palafrugell
Furio de l'Aygua Gélida
Torre del Moro
Pedra Blanca
Puig Gruig
Cala Tamaria
Tres Turons
Iglesia de Montrás
La Perica
Punta Tamaria
Puig Cucala
Santa Margarita
Puig Pedrosa
Cala Pedrosa
Puig Rodo
Puig d'els Frares
Punta Pedrosa
Montagut Petit
Puig Congre
Puig d'els Olls
Armadás
Llafranch
C. de S. Sebastian
Cala de Llafranch
Montagut
Calella
Turó Rial
Cala de Calella
Los Ullastres
Puig de las Negras
Cabo Roig
Puig Caragol
Torre y Turó Mirona
Puig d'en Rodó
Puig Parals
Alto del Terme
Roca la Sardana
Puig de las Bruixas
Puig Macaya
CARTA 306
Las Hormigas
Igl.a de Calonge
Ermita de San Daniel
Roca Negra
San Juan
Cala Fonda
Cala Alger y Castell
Torre Alxaña
Palamós
Ermita Cabrera
Cabo Gros
San Antonio
d'en Brosa
Mont del Pedró
CARTA 880
Riera de Calonge
Pta del Molino
Turó d'en Cama
Tª Valentina
Torre Celza
Turó de Gruañes
Pta de Tª Valentina
La Llosa o Laja de Palamós
d'en Roca
Cala Cañas
Cabo Roig
Guardia Civil de Playa de Aro
Pta Trumal o de los Esculls
Playa de Val de Aro
Pta Rojiza
Punta del Pinell
Laja La Llosa
Cala Concas
Pta d'en Pau
Mula
les Belelles
171
3° 00' W 1985 (7' E)

BOYA DE PALAMOS

Numero de Codigo : 171

Coordenadas Geograficas

Longitud : 3 gr. 10' 48'' E

Latitud : 41 gr. 49' 12'' N

Profundidad : 90 metros

Procedencia : R.E.M.R.O

Tipo de boya : Escalar (Waverider Datawell)

Tipo de datos : Procesados y registros brutos

Estado actual : En funcionamiento

ANALYSIS

PALAMO (41.8N 3.4E)
OCTOBER 1992

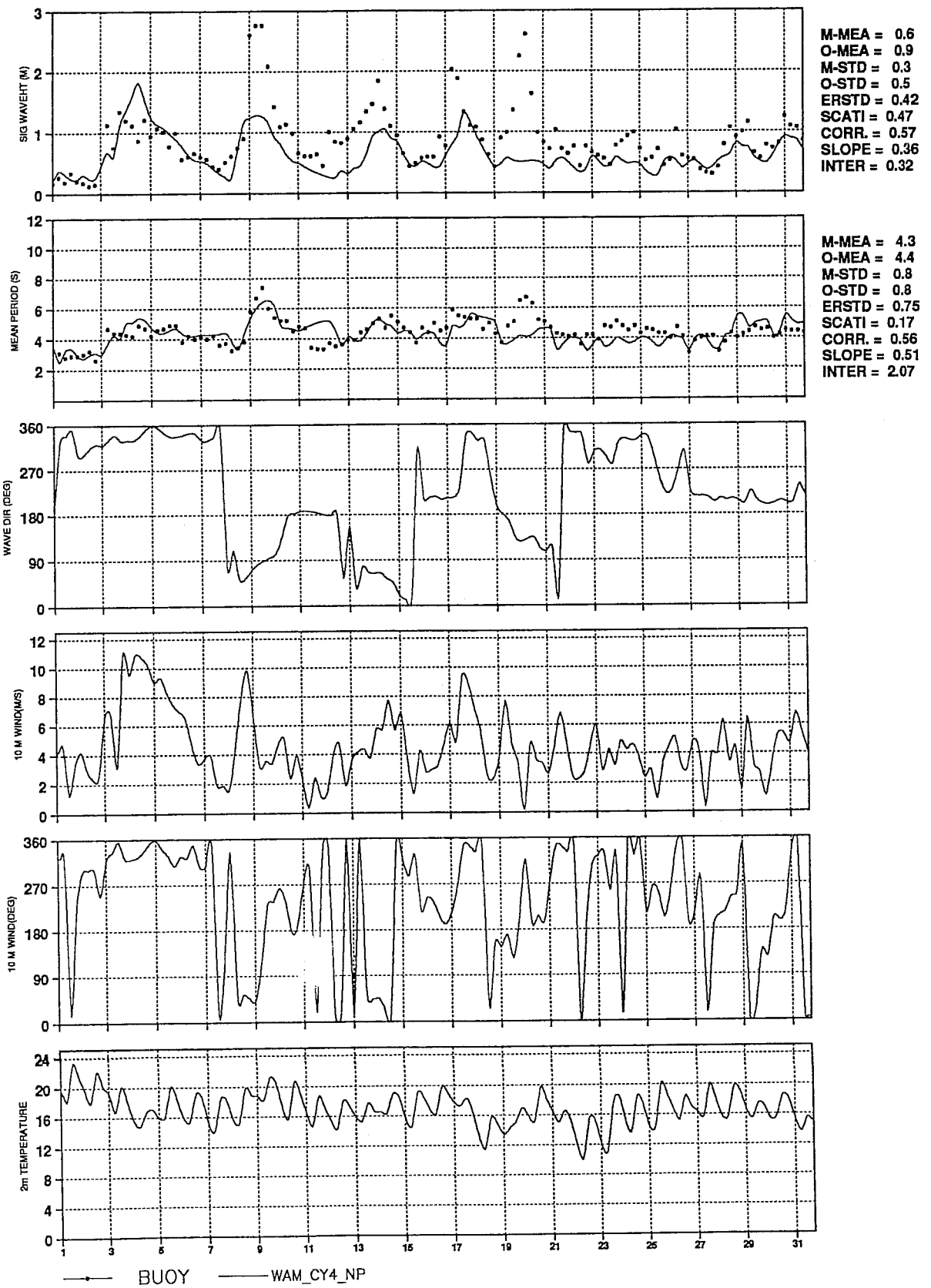

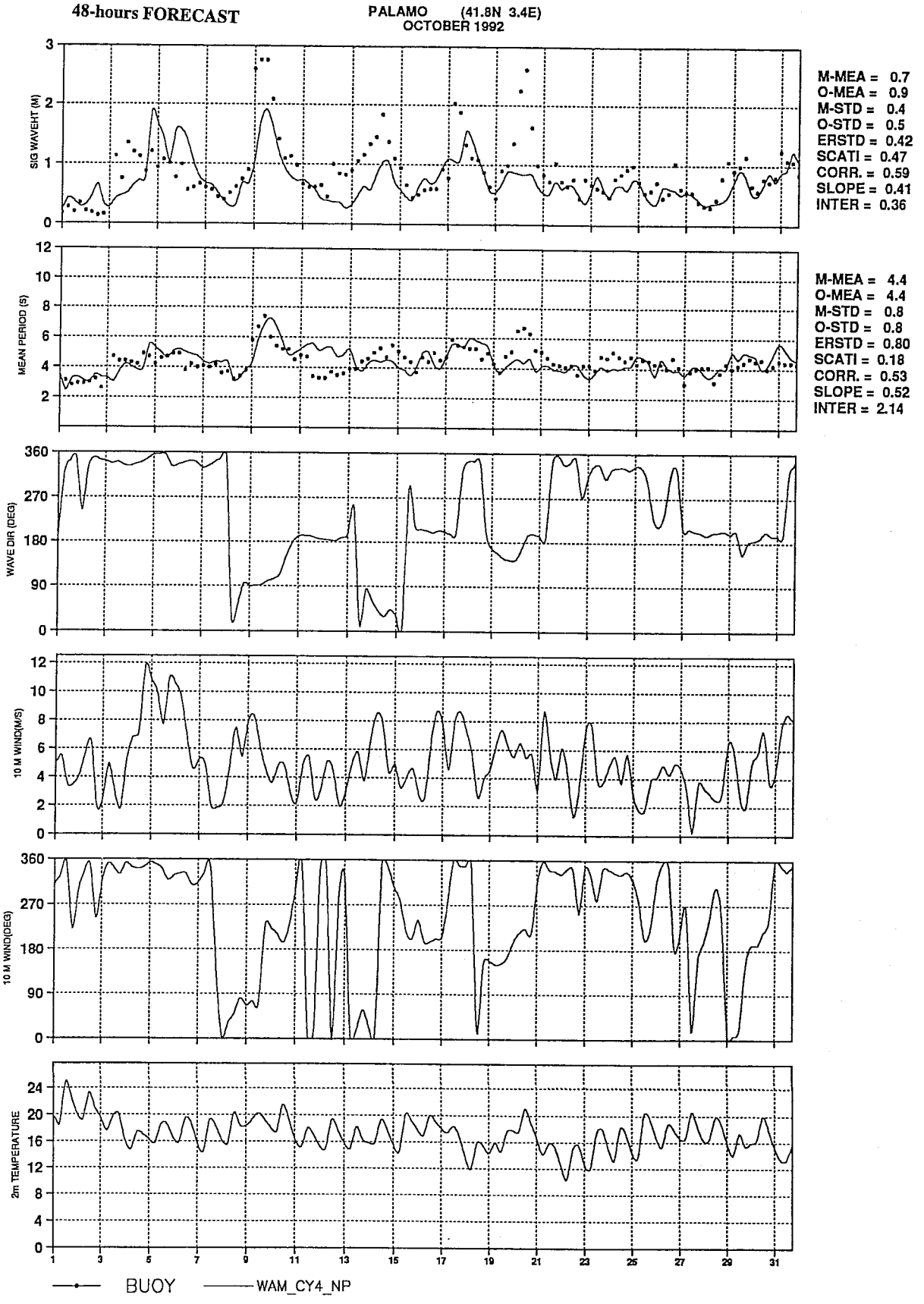
48-hours FORECAST
PALAMO (41.8N 3.4E)
OCTOBER 1992
SIG WAVEHT (M)
M-MEA = 0.7
O-MEA = 0.9
M-STD = 0.4
O-STD = 0.5
ERSTD = 0.42
SCATI = 0.47
CORR. = 0.59
SLOPE = 0.41
INTER = 0.36
MEAN PERIOD (S)
M-MEA = 4.4
O-MEA = 4.4
M-STD = 0.8
O-STD = 0.8
ERSTD = 0.80
SCATI = 0.18
CORR. = 0.53
SLOPE = 0.52
INTER = 2.14
WAVE DIR (DEG)
10 M WIND(M/S)
10 M WIND(DEG)
2m TEMPERATURE
BUOY
WAM_CY4_NP

ANALYSIS

PALAMO (41.8N 3.4E)
NOVEMBER 1992

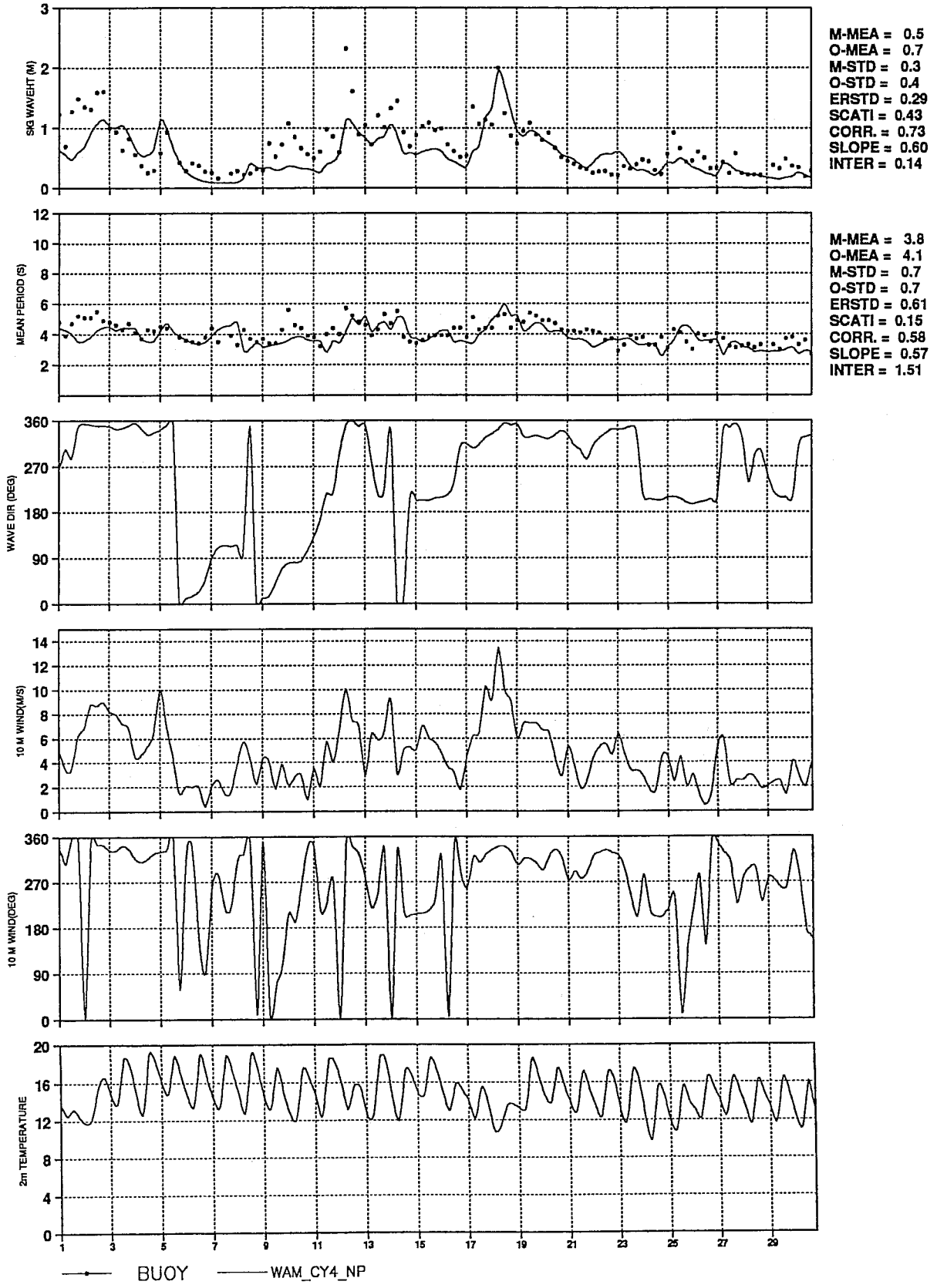

48-hours FORECAST

PALAMO (41.8N 3.4E)
NOVEMBER 1992

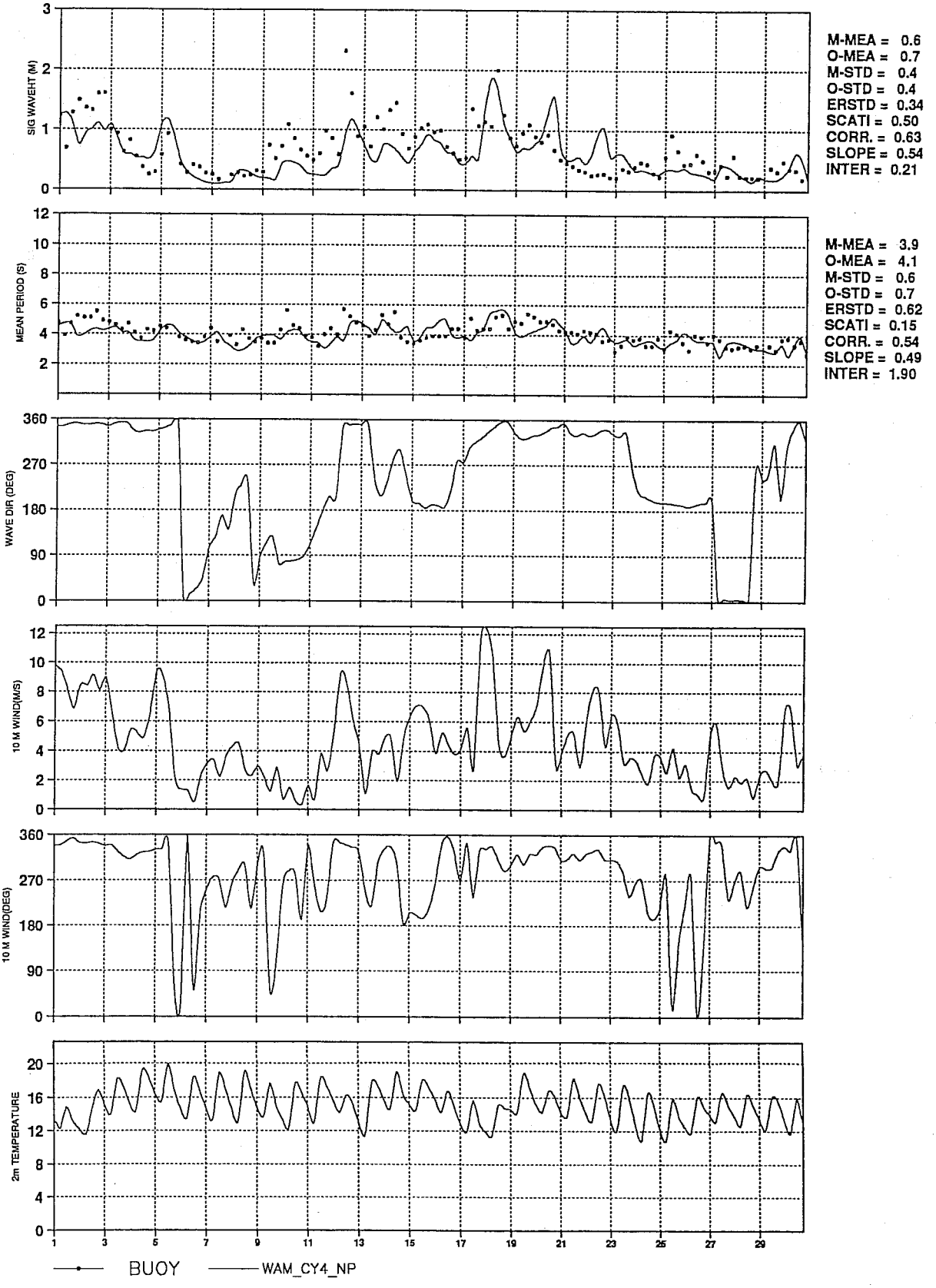

ANALYSIS

PALAMO (41.8N 3.4E)
DECEMBER 1992

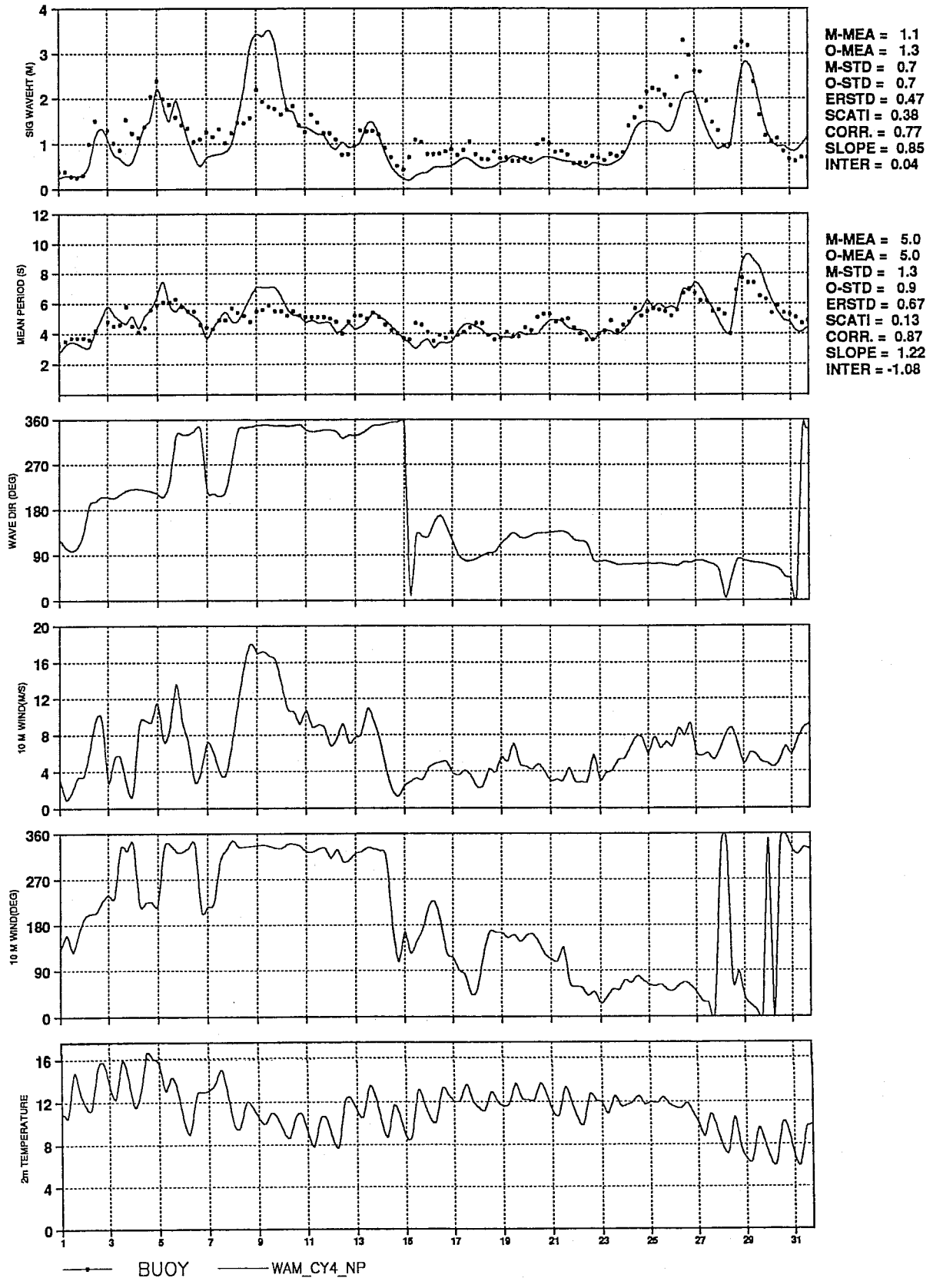

48-hours FORECAST

PALAMO (41.8N 3.4E)
DECEMBER 1992

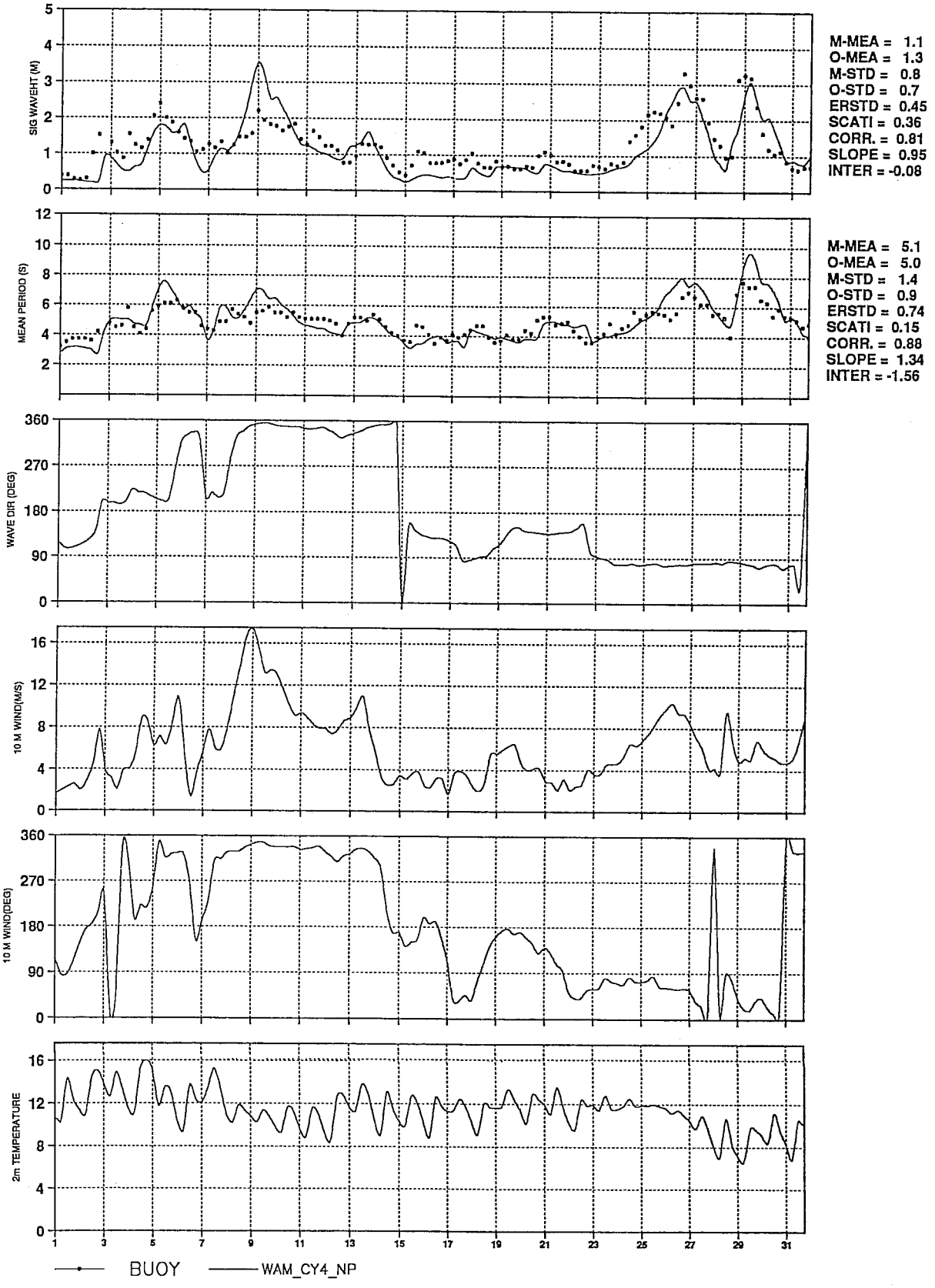

ANALYSIS

PALAMO (41.8N 3.4E)
JANUARY 1993

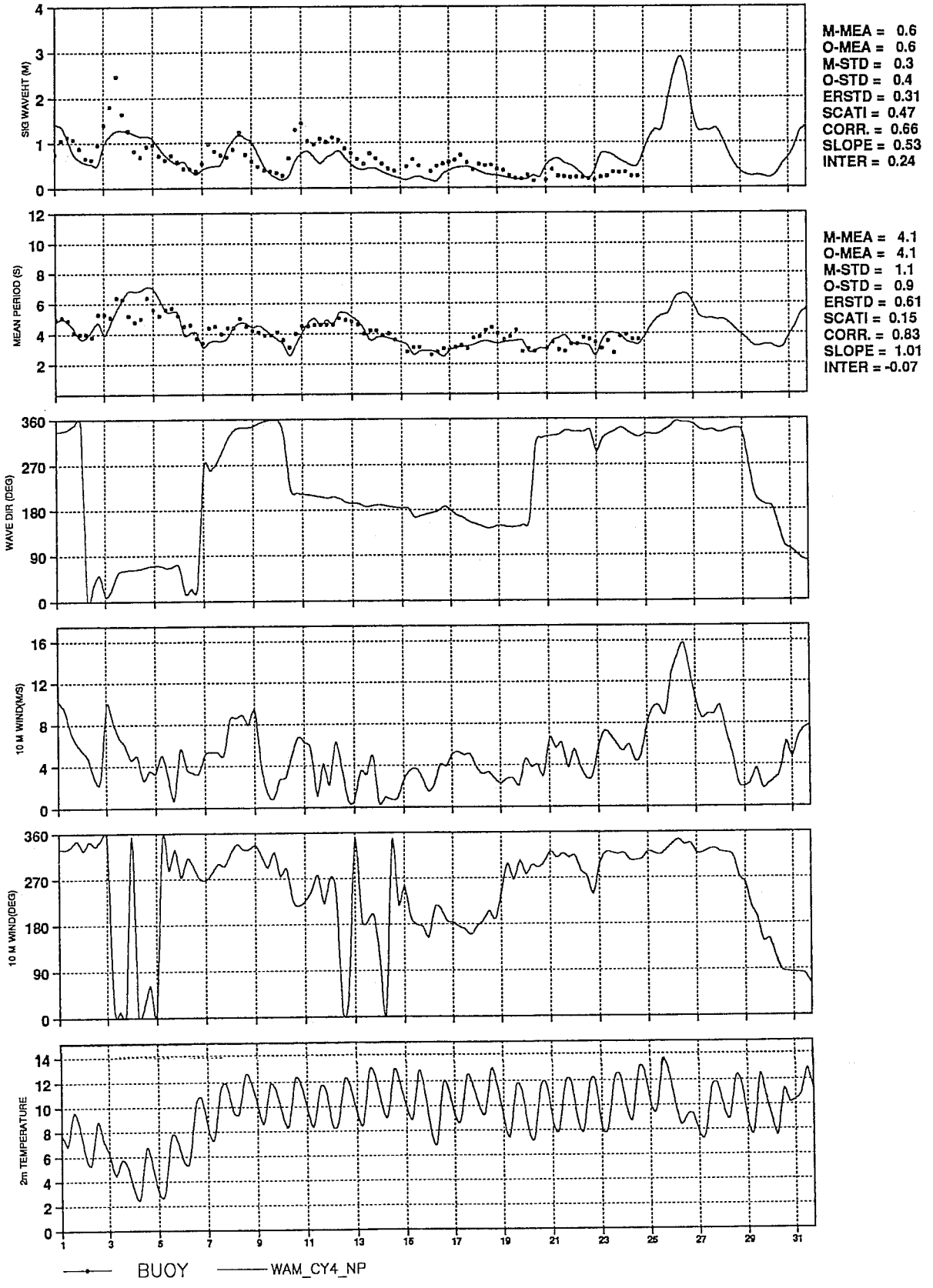

48-hours FORECAST

PALAMO (41.8N 3.4E)
JANUARY 1993

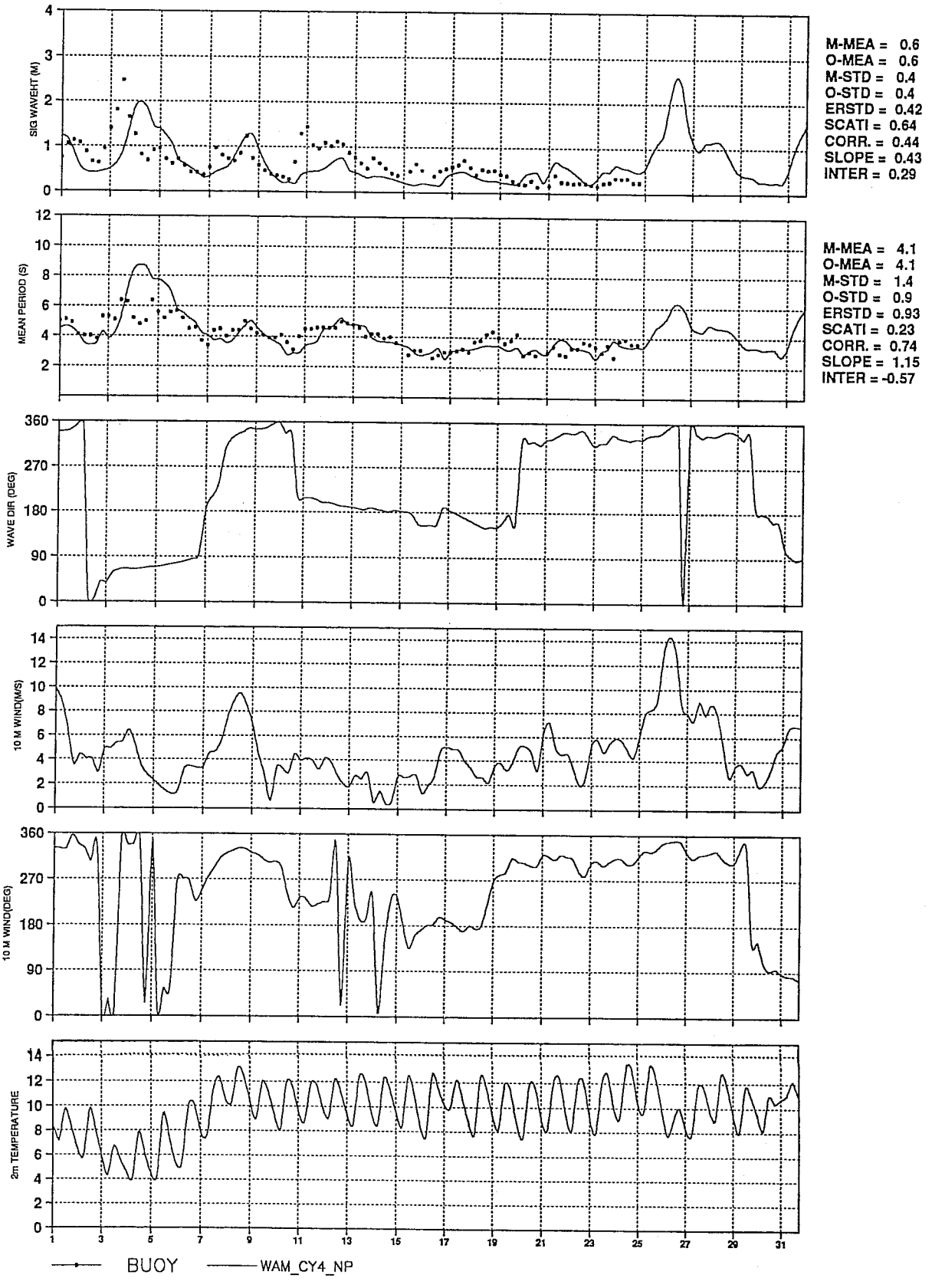

ANALYSIS

PALAMO (41.8N 3.4E)
FEBRUARY 1993

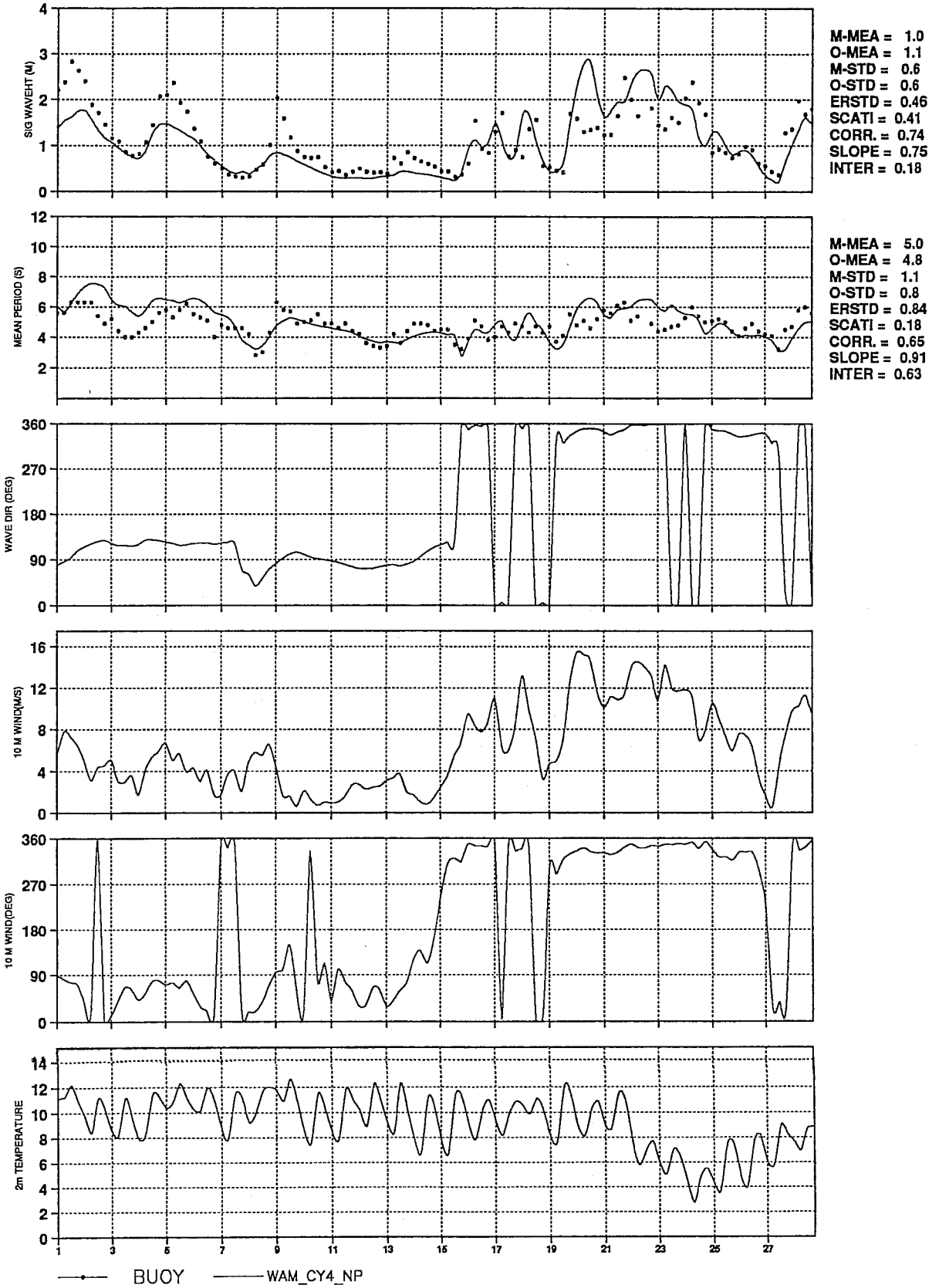

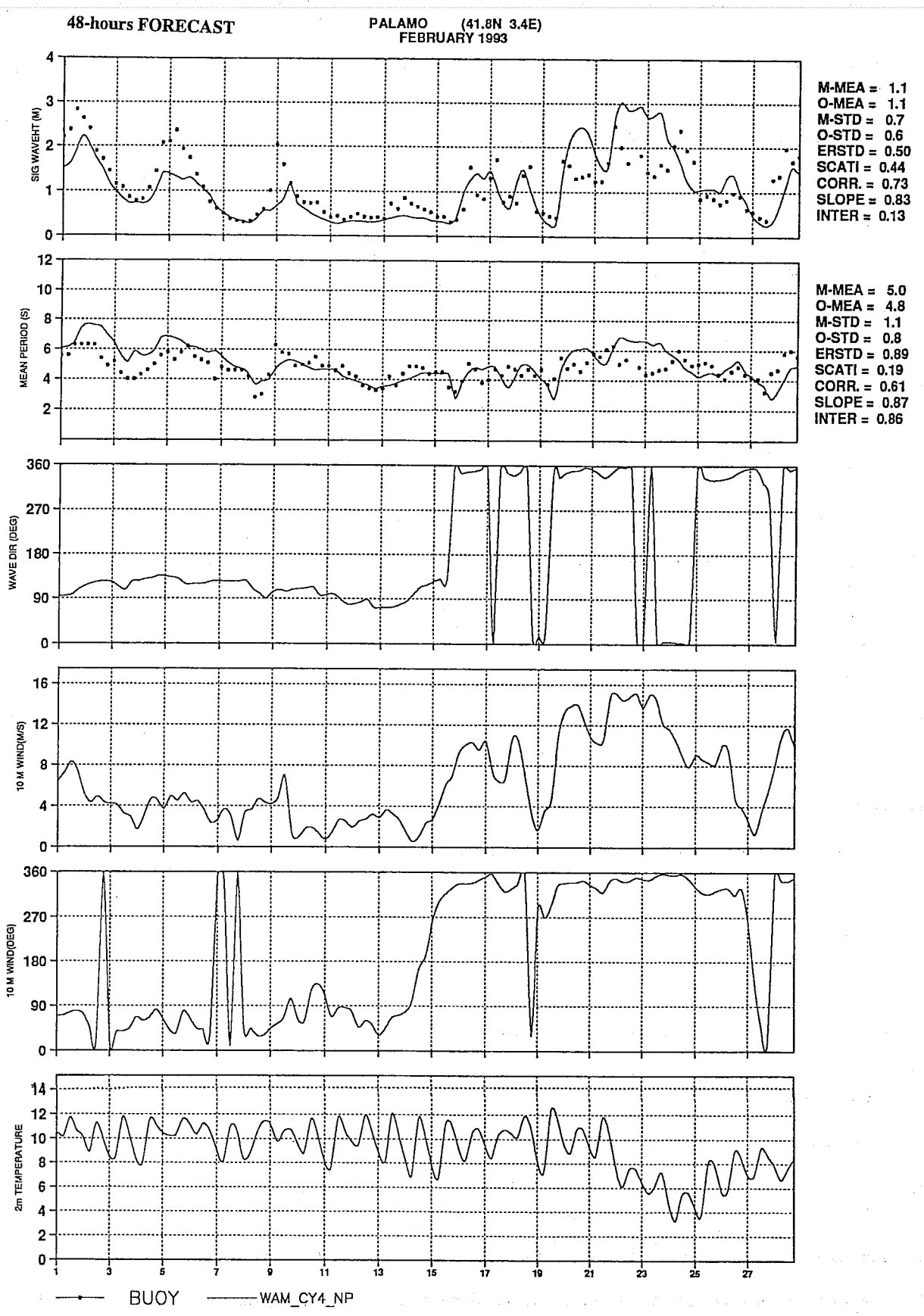
48-hours FORECAST
PALAMO (41.8N 3.4E)
FEBRUARY 1993
SIG WAVEHT (M)
M-MEA = 1.1
O-MEA = 1.1
M-STD = 0.7
O-STD = 0.6
ERSTD = 0.50
SCATI = 0.44
CORR. = 0.73
SLOPE = 0.83
INTER = 0.13
MEAN PERIOD (S)
M-MEA = 5.0
O-MEA = 4.8
M-STD = 1.1
O-STD = 0.8
ERSTD = 0.89
SCATI = 0.19
CORR. = 0.61
SLOPE = 0.87
INTER = 0.86
WAVE DIR (DEG)
10 M WIND(M/S)
10 M WIND(DEG)
2m TEMPERATURE
BUOY
WAM_CY4_NP

LIST OF ECMWF TECHNICAL REPORTS

1	A case study of a ten day forecast. (1976)	Arpe, K., L. Bengtsson, A. Hollingsworth, and Z. Janjić
2	The effect of arithmetic precision on some meteorological integrations. (1976)	Baede, A.P.M., D. Dent, and A. Hollingsworth
3	Mixed-radix Fourier transforms without reordering. (1977)	Temperton, C.
4	A model for medium range weather forecasts - adiabatic formulation. (1977)	Burridge, D.M., and J. Haseler
5	A study of some parameterisations of sub-grid processes in a baroclinic wave in a two dimensional model. (1977)	Hollingsworth, A.
6	The ECMWF analysis and data assimilation scheme: analysis of mass and wind field. (1977)	Lorenc, I. Rutherford and G. Larsen
7	A ten-day high-resolution non-adiabatic spectral integration; a comparative study. (1977)	Baede, A.P.M., and A.W. Hansen
8	On the asymptotic behaviour of simple stochastic-dynamic systems. (1977)	Wiin-Nielsen, A.
9	On balance requirements as initial conditions. (1978)	Wiin-Nielsen, A.
10	ECMWF model parameterisation of sub-grid scale processes. (1979)	Tiedtke, M., J.-F. Geleyn, A. Hollingsworth, and J.-F. Louis
11	Normal mode initialization for a multi-level grid-point model. (1979)	Temperton, C., and D.L. Williamson
12	Data assimilation experiments. (1978)	Seaman, R.
13	Comparison of medium range forecasts made with two parameterisation schemes. (1978)	Hollingsworth, A., K. Arpe, M. Tiedke, M. Capaldo, H. Sävijärvi, O. Åkesson, and J.A. Woods
14	On initial conditions for non-hydrostatic models. (1978)	Wiin-Nielsen, A.C.
15	Adiabatic formulation and organization of ECMWF's spectral model. (1979)	Baede, A.P.M., M. Jarraud, and U. Cubasch
16	Model studies of a developing boundary layer over the ocean. (1979)	Økland, H.
17	The response of a global barotropic model to forcing by large scale orography. (1980)	Quiby, J.
18	Confidence limits for verification and energetic studies. (1980)	Arpe, K.
19	A low order barotropic model on the sphere with orographic and newtonian forcing. (1980)	Källén, E.
20	A review of the normal mode initialization method. (1980)	Du Xing-yuan
21	The adjoint equation technique applied to meteorological problems. (1980)	Kontarev, G.
22	The use of empirical methods for mesoscale pressure forecasts. (1980)	Bergthorsson, P.
23	Comparison of medium range weather forecasts made with models using spectral or finite difference techniques in the horizontal. (1981)	Jarraud, M., C. Girard, and U. Cubasch
24	On the average errors of an ensemble of forecasts. (1981)	Derome, J.

25	On the atmospheric factors affecting the Levantine Sea. (1981)	Ozsoy, E.
26	Tropical influences on stationary wave motion in middle and high latitudes. (1981)	Simmons, A.J.
27	The energy budgets in North America, North Atlantic and Europe based on ECMWF analysis and forecasts. (1981)	Sävijärvi, H.
28	An energy and angular momentum conserving finite-difference scheme, hybrid coordinates and medium range weather forecasts. (1981)	Simmons, A.J., and R. Strüfing
29	Orographic influences on Mediterranean lee cyclogenesis and European blocking in a global numerical model. (1982)	Tibaldi, S. and A. Buzzi
30	Review and re-assessment of ECNET - A private network with open architecture. (1982)	Haag, A., Königshofer, F. and P. Quoilin
31	An investigation of the impact at middle and high latitudes of tropical forecast errors. (1982)	Haseler, J.
32	Short and medium range forecast differences between a spectral and grid point model. An extensive quasi-operational comparison. (1982)	Girard, C. and M. Jarraud
33	Numerical simulations of a case of blocking: The effects of orography and land-sea contrast. (1982)	Ji, L.R., and S. Tibaldi
34	The impact of cloud track wind data on global analyses and medium range forecasts. (1982)	Kållberg, P., S. Uppala, N. Gustafsson, and J. Pailleux
35	Energy budget calculations at ECMWF. Part 1: Analyses 1980-81. (1982)	Oriol, E.
36	Operational verification of ECMWF forecast fields and results for 1980-1981. (1983)	Nieminen, R.
37	High resolution experiments with the ECMWF model: a case study. (1983)	Dell'Osso, L.
38	The response of the ECMWF global model to the El-Niño anomaly in extended range prediction experiments. (1983)	Cubasch, U.
39	On the parameterisation of vertical diffusion in large-scale atmospheric models. (1983)	Manton, M.J.
40	Spectral characteristics of the ECMWF objective analysis system. (1983)	Daley, R.
41	Systematic errors in the baroclinic waves of the ECMWF. (1984)	Klinker, E., and M. Capaldo
42	On long stationary and transient atmospheric waves. (1984)	Wiin-Nielsen, A.C.
43	A new convective adjustment. (1984)	Betts, A.K., and M.J. Miller
44	Numerical experiments on the simulation of the 1979 Asian summer monsoon. (1984)	Mohanty, U.C., R.P. Pearce and M. Tiedtke
45	The effect of mechanical forcing on the formation of a mesoscale vortex. (1984)	Guo-xiong Wu and Shou-jun Chen
46	Cloud prediction in the ECMWF model. (1985)	Slingo, J., and B. Ritter
47	Impact of aircraft wind data on ECMWF analyses and forecasts during the FGGE period, 8-19 November. (1985)	Baede, A.P.M., P. Kållberg, and S. Uppala

48	A numerical case study of East Asian coastal cyclogenesis. (1985)	Chen, Shou-jun and L. Dell'Osso
49	A study of the predictability of the ECMWF operational forecast model in the tropics. (1985)	Kanamitsu, M.
50	On the development of orographic. (1985)	Radinović, D.
51	Climatology and systematic error of rainfall forecasts at ECMWF. (1985)	Molteni, F., and S. Tibaldi
52	Impact of modified physical processes on the tropical simulation in the ECMWF model. (1985)	Mohanty, U.C., J.M. Slingo and M. Tiedtke
53	The performance and systematic errors of the ECMWF tropical forecasts (1982-1984). (1985)	Heckley, W.A.
54	Finite element schemes for the vertical discretization of the ECMWF forecast model using linear elements. (1986)	Burridge, D.M., J. Steppeler, and R. Strüfing
55	Finite element schemes for the vertical discretization of the ECMWF forecast model using quadratic and cubic elements. (1986)	Steppeler, J.
56	Sensitivity of medium-range weather forecasts to the use of an envelope orography. (1986)	Jarraud, M., A.J. Simmons and M. Kanamitsu
57	Zonal diagnostics of the ECMWF operational analyses and forecasts. (1986)	Branković, Č.
58	An evaluation of the performance of the ECMWF operational forecasting system in analysing and forecasting tropical easterly disturbances. Part 1: Synoptic investigation. (1986)	Reed, R.J., A. Hollingsworth, W.A. Heckley and F. Delsol
59	Diabatic nonlinear normal mode initialisation for a spectral model with a hybrid vertical coordinate. (1987)	Wergen, W.
60	An evaluation of the performance of the ECMWF operational forecasting system in analysing and forecasting tropical easterly wave disturbances. Part 2: Spectral investigation. (1987)	Reed, R.J., E. Klinker and A. Hollingsworth
61	Empirical orthogonal function analysis in the zonal and eddy components of 500 mb height fields in the Northern extratropics. (1987)	Molteni, F.
62	Atmospheric effective angular momentum functions for 1986-1987. (1989)	Sakellarides, G.
63	A verification study of the global WAM model December 1987 - November 1988. (1989)	Zambresky, L.
64	Impact of a change of radiation transfer scheme in the ECMWF model. (1989)	Morcrette, J-J.
65	The ECMWF analysis-forecast system during AMEX. (1990)	Puri, K., P. Lönnberg and M. Miller
66	The calculation of geopotential and the pressure gradient in the ECMWF atmospheric model: Influence on the simulation of the polar atmosphere and on temperature analyses (1990)	Simmons, A.J. and Chen Jiabin
67	Assimilation of altimeter data in a global third generation wave model (1992)	Lionello, P., H. Günther and P. Janssen
68	Implementation of a third generation ocean wave model at the European Centre for Medium-Range Weather Forecasts (1992)	Günther, H., P. Lionello, P.A.E.M. Janssen et al.
69	A preliminary study of the impact of C-band scatterometer wind data on global scale numerical weather prediction (1992)	Hoffman, R.N.

70	Scientific assessment of the prospects for seasonal forecasting: a European perspective March 1993	Palmer, T.N. and D.L.T. Anderson
71	Results with a coupled wind-wave model February 1994	Janssen, P.A.E.M.
72	Implementation of the semi-Lagrangian method in a high resolution version of the ECMWF forecast model June 1994	Ritchie, H., C. Temperton, A. Simmons, M. Hortal, T. Davies, D. Dent and M. Hamrud
73	Raw HIRS/2 radiances and model simulations in the presence of clouds September 1994	Rizzi, R.